16

Nissen, S. E., T. R. Carr, K. J. Marfurt, and E. C. Sullivan, 2009, Using 3-D seismic volumetric curvature attributes to identify fracture trends in a depleted Mississippian carbonate reservoir: Implications for assessing candidates for CO_2 sequestration, *in* M. Grobe, J. C. Pashin, and R. L. Dodge, eds., Carbon dioxide sequestration in geological media—State of the science: AAPG Studies in Geology 59, p. 297–319.

Using 3-D Seismic Volumetric Curvature Attributes to Identify Fracture Trends in a Depleted Mississippian Carbonate Reservoir: Implications for Assessing Candidates for CO_2 Sequestration

Susan E. Nissen
Consultant, McLouth, Kansas, U.S.A.

Timothy R. Carr
Department of Geology and Geography, West Virginia University, Morgantown, West Virginia, U.S.A.

Kurt J. Marfurt
College of Earth and Energy, University of Oklahoma, Norman, Oklahoma, U.S.A.

E. Charlotte Sullivan
Pacific Northwest National Laboratories, Richland, Washington, U.S.A.

ABSTRACT

The widespread Western Interior Plains aquifer system of the central United States provides a significant potential for sequestration of CO_2 in a deep saline formation. In Kansas, several severely depleted Mississippian petroleum reservoirs sit at the top of this aquifer system. The reservoirs are primarily multilayered shallow-shelf carbonates with strong water drives. Fluid flow is strongly influenced by natural fractures, which were solution enhanced by subaerial karst on a Mississippian–Pennsylvanian regional unconformity. We show that three-dimensional (3-D) seismic volumetric reflector curvature attributes can reveal subtle lineaments related to these fractures. Volumetric curvature attributes applied to a 3-D seismic survey over a Mississippian oil reservoir in Dickman field, Ness County, Kansas, reveal two main lineament orientations, N45°E and N45°W. The northeast-trending lineaments parallel a down-to-the-north fault

Copyright ©2009 by The American Association of Petroleum Geologists.
DOI:10.1306/13171245St591798

at the northwestern corner of the seismic survey and have greater length and continuity than the northwest-trending lineaments. Geologic analysis and production data suggest that the northeast-trending lineaments are related to debris-, clay-, and silt-filled fractures that serve as barriers to fluid flow, whereas the northwest-trending lineaments are related to open fractures that channel water from the underlying aquifer. The discrimination of open versus sealed fractures within and above potential CO_2 sequestration reservoirs is critical for managing the injection and storage of CO_2 and for evaluating the integrity of the overlying seal. Three-dimensional seismic volumetric curvature helps to locate fractures and is a potentially important tool in the selection and evaluation of geologic sequestration sites.

INTRODUCTION

Mature and supermature oil and gas fields and deep saline formations in the United States are two targets for geologic sequestration of CO_2 (U.S. Department of Energy, 2007). Many of these oil and gas reservoirs and aquifers contain natural fractures (e.g., Holtz et al., 1999; White et al., 2004; Friedmann and Stamp, 2006). The discrimination of open versus sealed fractures within and above the reservoirs or aquifers is critical for the management of injection and storage of CO_2 and for evaluating the integrity of the overlying seal. However, geologic information about mature and supermature oil and gas fields typically comes from drill cuttings and limited wireline logs from vertical wells. Even less information is available for many saline aquifers, which are not drilled as extensively as oil and gas fields. As a result, accurate identification of the lateral distribution of fractures that influence fluid flow in and above potential CO_2 sequestration reservoirs, and that therefore impact sequestration potential and long-term leakage risks, is difficult. Three-dimensional (3-D) seismic data, analyzed using modern 3-D seismic attributes such as volumetric curvature, provide a means for identifying the spatial distribution and trends of major fractures or fissures.

We apply 3-D seismic volumetric curvature attributes to a 3-D seismic survey over a typical supermature field in Kansas (Dickman field), which also lies atop a major saline aquifer, to reveal subtle lineaments that are related to fractures in the reservoir and underlying aquifer. Our attribute interpretations are integrated with geologic and engineering information to improve our understanding of how the fractures affect lateral fluid movement.

We begin with a summary of the regional geology and structural setting of the study area, followed by a description of the reservoir at Dickman field and the function of fractures in the reservoir. Next, we introduce the 3-D seismic data and describe our fracture-mapping methodology using volumetric curvature. We calibrate fractures to production data through the introduction of a novel correlation technique that considers not only the strike of fracture-related lineaments, but also the distance of the lineaments from the wells. We conclude with suggestions about how this work could be applied in the evaluation and management of geologic CO_2 sequestration reservoirs.

REGIONAL GEOLOGY

The lower Paleozoic Ozark Plateau aquifer system is a widespread regional-scale aquifer system that extends across parts of nine states (Figure 1A). The freshwater component of the system, primarily located in Missouri and Arkansas, is known as the Ozark Plateau aquifer system, whereas the saline component is referred to as the Western Interior Plains aquifer system (Jorgensen, 1989; Jorgensen et al., 1993, 1996). The saline Western Interior Plains aquifer system is a potential site for sequestration of large quantities of CO_2.

A generalized stratigraphic section for Kansas (Figure 1B) shows that the Ozark Plateau aquifer system is divided into a lower unit of Cambrian sandstone and Cambrian–Ordovician carbonate and an upper unit of Mississippian carbonate. A confining unit of low permeability carbonate and shale separates these two aquifer units. The present study focuses on the upper (Mississippian) aquifer unit in Ness County, Kansas.

The Mississippian aquifer unit is associated with oil and gas reservoirs throughout Kansas (Figure 2). Approximately 1 billion bbl of oil have been produced from the Mississippian in the state, accounting for approximately 19% of total Kansas oil production (Carr, 1994). Most of the Mississippian reservoirs are supermature, but considerable amounts of petroleum remain to be produced using enhanced recovery techniques, such as CO_2 flooding. Depleted petroleum reservoirs are expected to be good candidates for CO_2 sequestration because of their proven seal integrity.

In Kansas, the Mississippian aquifer unit is composed primarily of naturally fractured shallow-shelf carbonates of Osagian to Chesterian age. The aquifer unit is immediately underlain by low-porosity and low-permeability

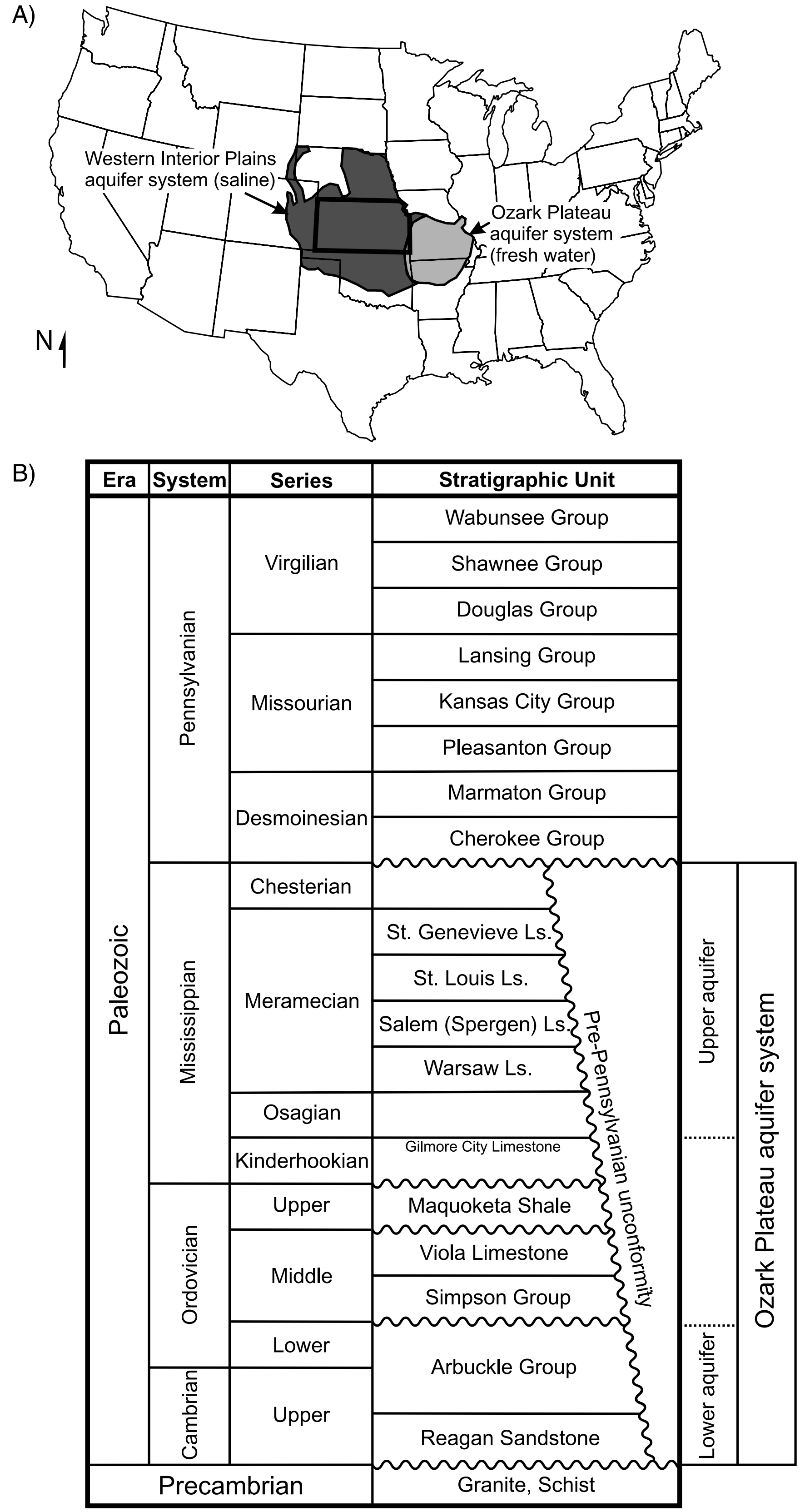

FIGURE 1. (A) Map of the United States, showing the regional extent of the Ozark plateau aquifer system (modified from Jorgensen et al., 1993). The freshwater (Ozark Plateau) component of the aquifer is shaded in light gray, whereas the saline (Western Interior Plains) component is shaded in dark gray. Kansas is highlighted with a heavy black line. The saline Western Interior Plains aquifer has considerable potential for the sequestration of anthropogenic CO_2. (B) Generalized stratigraphic column for central Kansas (modified from Cansler, 2000), showing the stratigraphic position of the Ozark Plateau aquifer system.

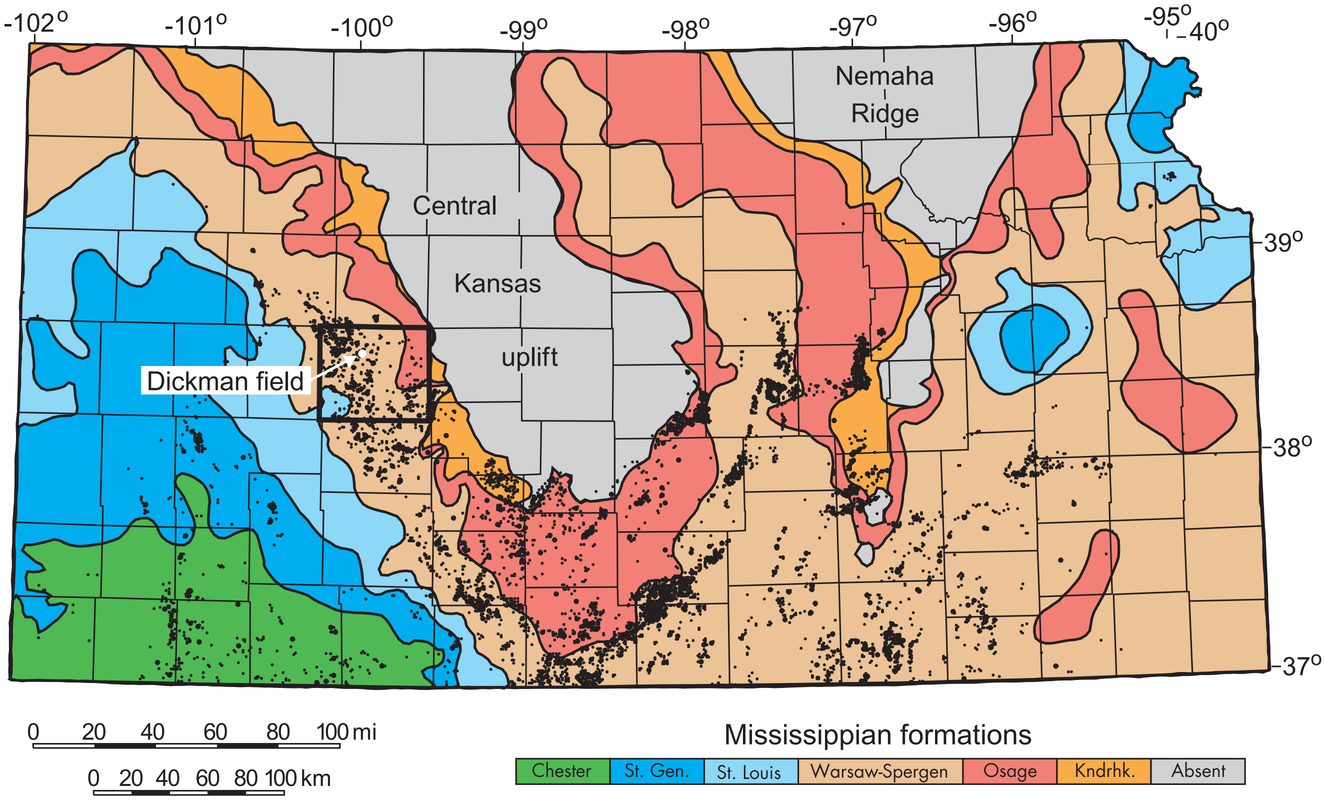

FIGURE 2. Map of the Mississippian subcrop in Kansas (modified from Merriam, 1963). Black dots indicate Mississippian oil production. Ness County is outlined by the heavy black box. White dot shows the location of Dickman field. St. Gen. = Sainte Generiere; Kndrhk. = Kinderhook.

Kinderhookian carbonate and is unconformably overlain by Pennsylvanian shale of the Cherokee Group, which serves as a confining unit for the aquifer. The Mississippian aquifer unit is present over most of Kansas, except on the crests of the Central Kansas uplift and the Nemaha Ridge (Figure 2). These uplifted terranes were eroded in the post-Mississippian to pre-Desmoinesian (Merriam, 1963), forming a pronounced regional unconformity surface. The top of the Mississippian aquifer unit was subaerially exposed and modified by extensive karst prior to deposition of the Pennsylvanian sediments. Goebel (1966), Nodine-Zeller (1981), and Montgomery et al. (2000), among others, reported examples of karst development in the Mississippian rocks beneath the pre-Pennsylvanian unconformity surface at locations throughout western Kansas, including Ness County, which is situated on the western flank of the Central Kansas uplift. Solution enhancement of natural fractures, instead of cavern formation, appears to have been the predominant karst process. Oil and water production in the Mississippian reservoirs of western Kansas is strongly influenced by these solution-enhanced fractures (e.g., Montgomery et al., 2000; Bhattacharya et al., 2005).

We created a subsea depth map of the top of the Mississippian (equivalent to the pre-Pennsylvanian unconformity surface) for Ness County, Kansas (Figure 3), from 4324 wells with publicly available stratigraphic interpretations of the top of the Mississippian (Kansas Geological Survey, 2008). Generally, the unconformity surface deepens toward the southeast. Superimposed on this dipping surface are regional structural highs, which may be related to basement faulting (e.g., Montgomery et al., 2000). The structures are primarily northeast trending, although a northwest structural trend exists in the northeastern part of the county.

A map of dip magnitude (Figure 4A) calculated from the top of the Mississippian surface highlights the major regional structural trends for Ness County. Although local topographic features related to karst will produce relatively high dip magnitudes, linear areas of high dip probably represent deep-seated faults. These deep-seated faults likely control the orientations of fracture swarms in the Mississippian rocks. Lineaments interpreted from the dip map show a regional structural fabric dominated by northeasterly and northwesterly trends (Figure 4B).

Northeasterly and northwesterly trends are also seen in the regional residual Bouguer gravity map (Figure 5) and the aeromagnetic map (Figure 6) of Ness County. Gravity and magnetic maps reflect structural and compositional variations in the Precambrian basement of Kansas (e.g., Yarger, 1983; Lam and Yarger, 1989). The similarity

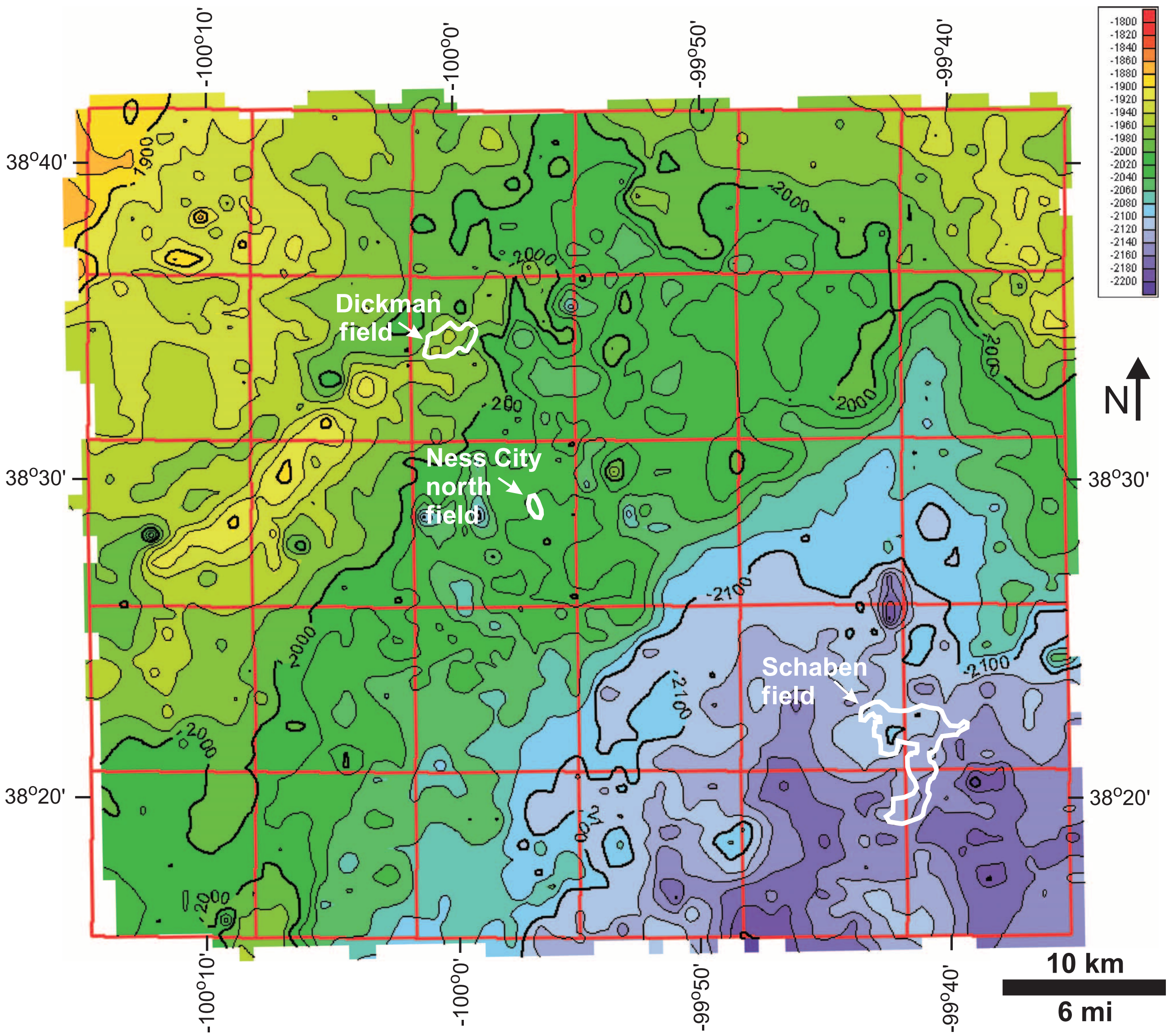

FIGURE 3. Map showing the depth below sea level of the top of the Mississippian (pre-Pennsylvanian unconformity surface) for Ness County, Kansas, created from 4324 publicly available well picks. Contour interval = 6 m (20 ft). Oil fields discussed in the text are outlined in white. Red lines are township boundaries.

in trend between Mississippian structural features and the features seen on the gravity and aeromagnetic maps suggests a relation between the configuration of the top of the Mississippian and basement structure.

DICKMAN FIELD

Dickman field (Figure 7), located in northern Ness County, Kansas, is a typical supermature Mississippian reservoir. This field was discovered in 1962 and has subsequently produced nearly 1.7 million bbl of oil, primarily from the Mississippian, although minor production from the Pennsylvanian Marmaton and Cherokee groups exists (Figure 1B). Dickman field sits at the northern end of a northeast-trending structural high that cuts through western Ness County (Figure 3). The field is also located just to the south of an intersection between a northeast-trending lineament and a northwest-trending lineament on the Mississippian dip magnitude map (Figure 4A).

In Dickman field, Pennsylvanian (Desmoinesian) strata unconformably overlie Mississippian reservoir rocks (chiefly dolomite and cherty dolomite) of the Meramecian Spergen and Warsaw limestones (Figures 1, 2). The Mississippian reservoir in Dickman field is composed of shallow-shelf carbonates (mudstone to packstone lithofacies, with moldic porosity). The top of the Mississippian reservoir sits from 0 to 3 m (0 to 10 ft) below the pre-Pennsylvanian unconformity surface and up to 11 m (35 ft) above the oil-water contact. The reservoir has a

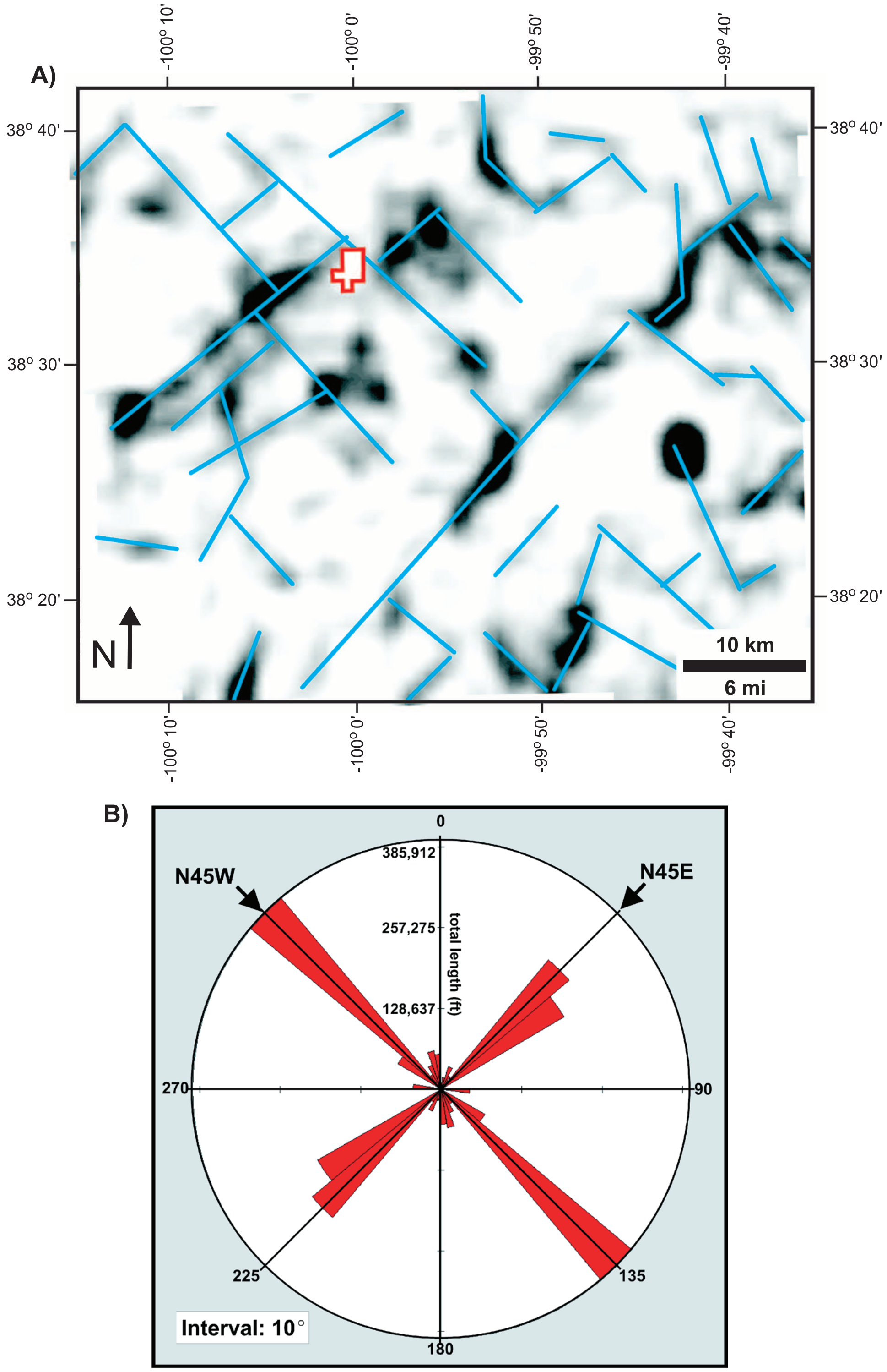

Figure 4. (A) Map of the dip magnitude calculated from the top of Mississippian surface shown in Figure 3. Black indicates high dip. Interpreted lineaments are shown in blue. High dip magnitude lineaments are likely to represent either faults or sediment drape over deeper faults. The location of the Dickman field 3-D seismic survey is outlined in red. (B) Length-azimuth rose diagram of lineaments interpreted from the map in panel A.

strong bottom water drive and high water-cut production (greater than 94%). The reservoir's bottom water drive is supported by the Mississippian aquifer unit of the Western Interior Plains aquifer system, which extends approximately 40–55 m (130–180 ft) below the reservoir to the low-porosity and low-permeability Kinderhookian Gilmore City Limestone (Figure 8).

Seven wells in Dickman field have been cored (Figure 7). The cores show that the Mississippian reservoir contains solution-enlarged natural fractures, primarily vertical in orientation (Figure 9). Some of the fractures are clay filled. Three of the cored wells (Dickman 5, Elmore 1, and Dickman 2) also appear to have penetrated rubble near the pre-Pennsylvanian unconformity surface.

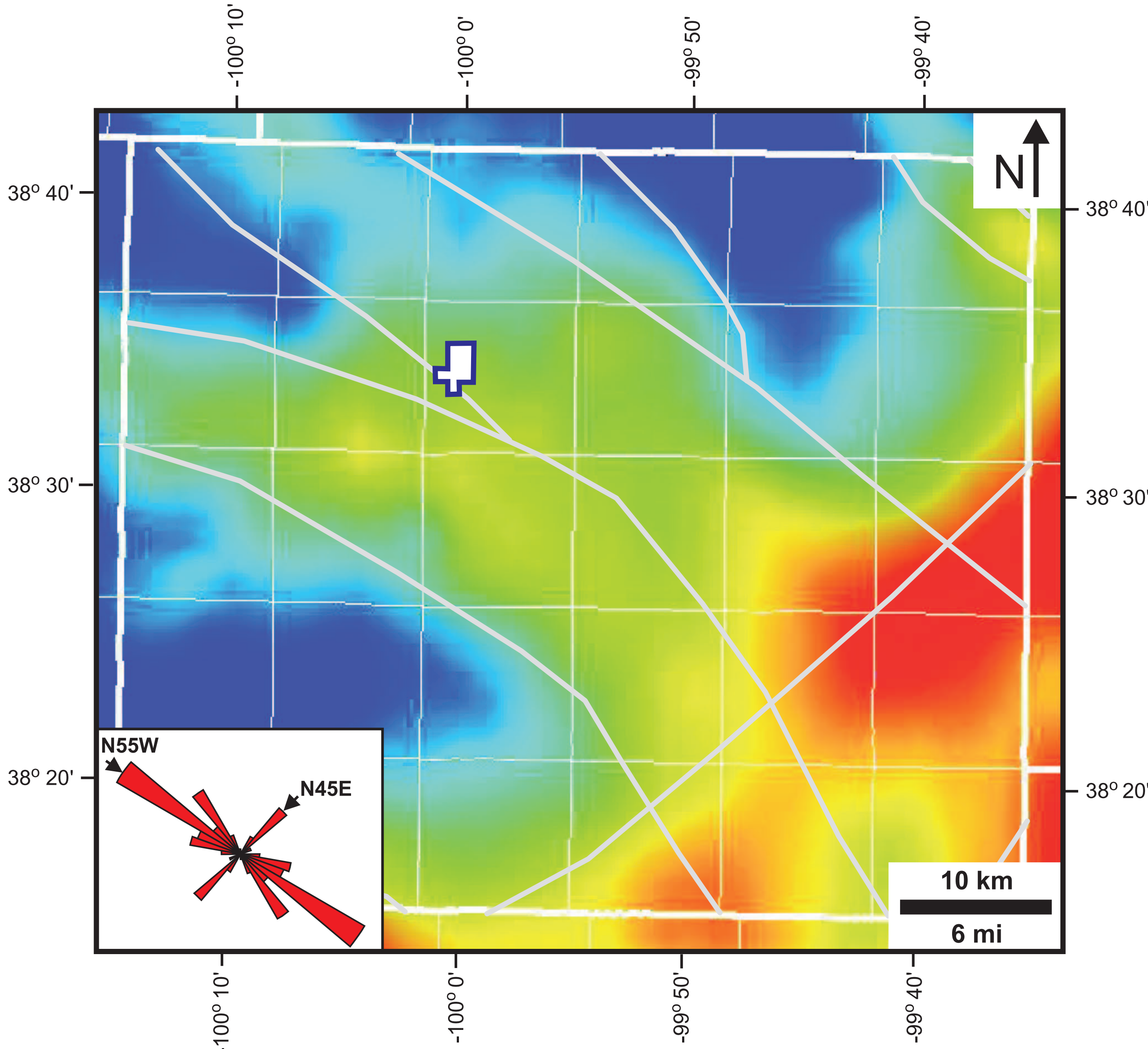

Figure 5. Residual Bouguer gravity map for Ness County, Kansas, with regional gravity lineaments from Kruger (1997) superimposed in gray. Blue represents lowest values and red represents highest values. The location of the Dickman field 3-D seismic survey is outlined in blue. Thin white lines are township boundaries and heavy white lines are county boundaries. Inset: Length-azimuth rose diagram of Ness County regional gravity lineaments.

The rubble deposits lack sediment and textural characteristics indicative of large-scale cavern collapse as described by Loucks et al. (2004) but, instead, are suggestive of large (somewhat wider than the wellbore) solution-enhanced fractures filled by clay, silt, and Mississippian rock debris. In Dickman 5, a zone of reworked Mississippian dolomite is present above the pre-Pennsylvanian unconformity surface. Dickman 5 also encountered the top of the Mississippian at a depth deeper than expected, with the Warsaw Limestone sitting directly below the unconformity surface, as compared to the younger Spergen Limestone that is present in most of the other wells in Dickman field (Figure 10). We infer that the Dickman 5 well is located directly in a large solution-enhanced fracture, which has been filled with Mississippian rubble. In the core from Elmore 1, the contact between the Mississippian dolomite and the overlying Pennsylvanian shale is at an angle of 45°, and clay or shale interbedded with the dolomite within the uppermost 1.5 m (5 ft) of the Mississippian shows the same discordance. Dickman 2 also shows an angular contact between shale and dolomite 2.1 m (7 ft) below the top of the Mississippian. The angular nature of the contacts between shale and dolomite suggests that the Elmore 1 and Dickman 2 wells

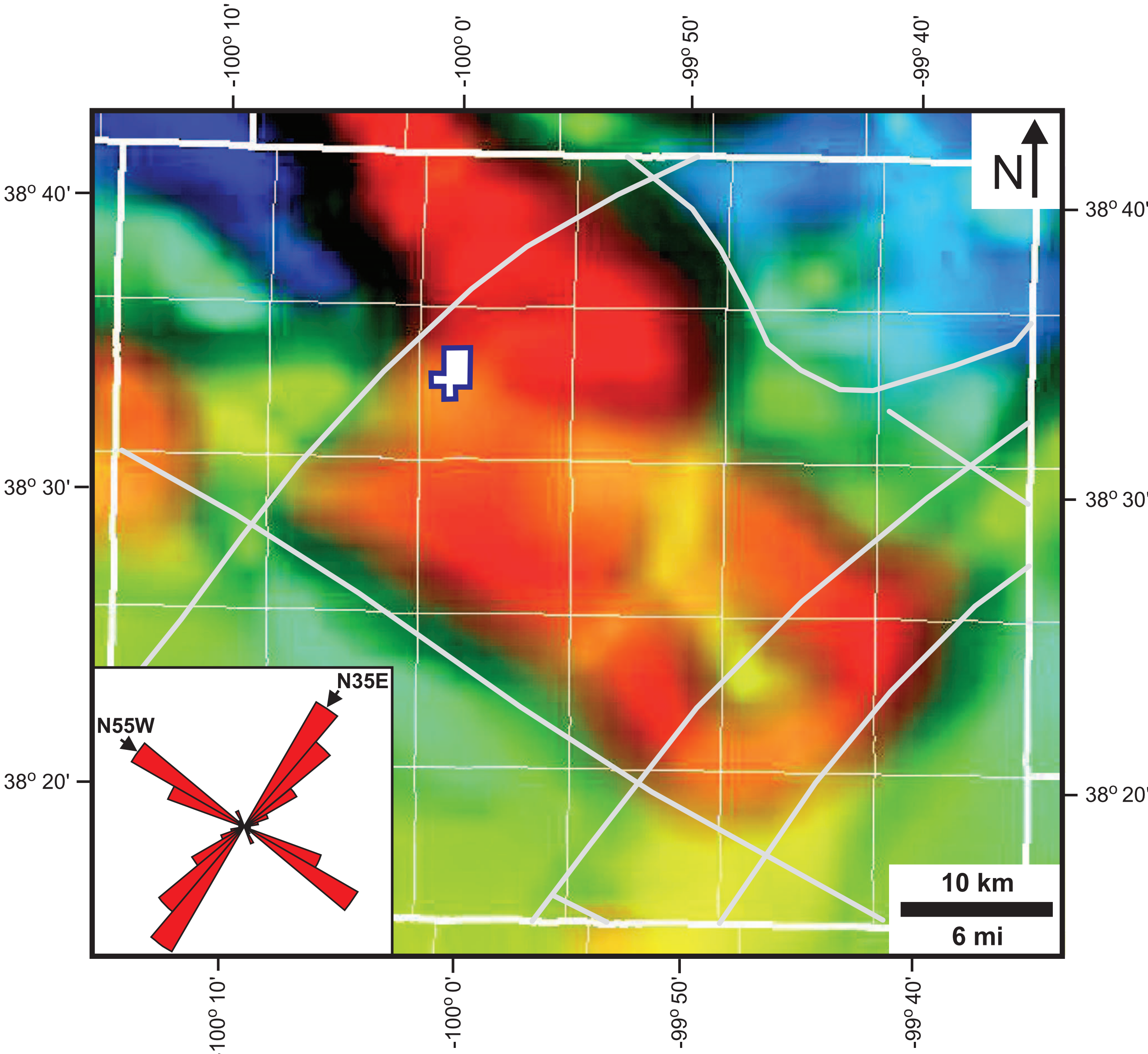

FIGURE 6. Aeromagnetic map for Ness County, Kansas, with regional magnetic lineaments from Kruger (1997) superimposed in gray. Blue represents lowest values and red represents highest values. The location of the Dickman field 3-D seismic survey is outlined in blue. Thin white lines are township boundaries and heavy white lines are county boundaries. Inset: Length-azimuth rose diagram of Ness County regional magnetic lineaments.

have encountered rotated blocks of Mississippian dolomite that form part of the debris fill of large solution-enhanced fractures.

In general, fractures that were solution enhanced by post-Mississippian karst to form wide fissures are likely to be filled by a combination of Pennsylvanian fine-grained material of the Cherokee Group and weathered Mississippian rock debris, reflecting deposition of Pennsylvanian sediment coincident with the accumulation of collapsed rubble from the sides of the fissures. Although the wells in Dickman field contain evidence for large fractures filled by debris and fine-grained sediments, the dimensions, extent, and trend of these potential fractures cannot be determined from core or other well data.

THE ROLE OF FRACTURES IN THE MISSISSIPPIAN RESERVOIR

Franseen et al. (1998) studied the Osagian reservoir in Schaben field, Ness County, Kansas (Figure 3), and

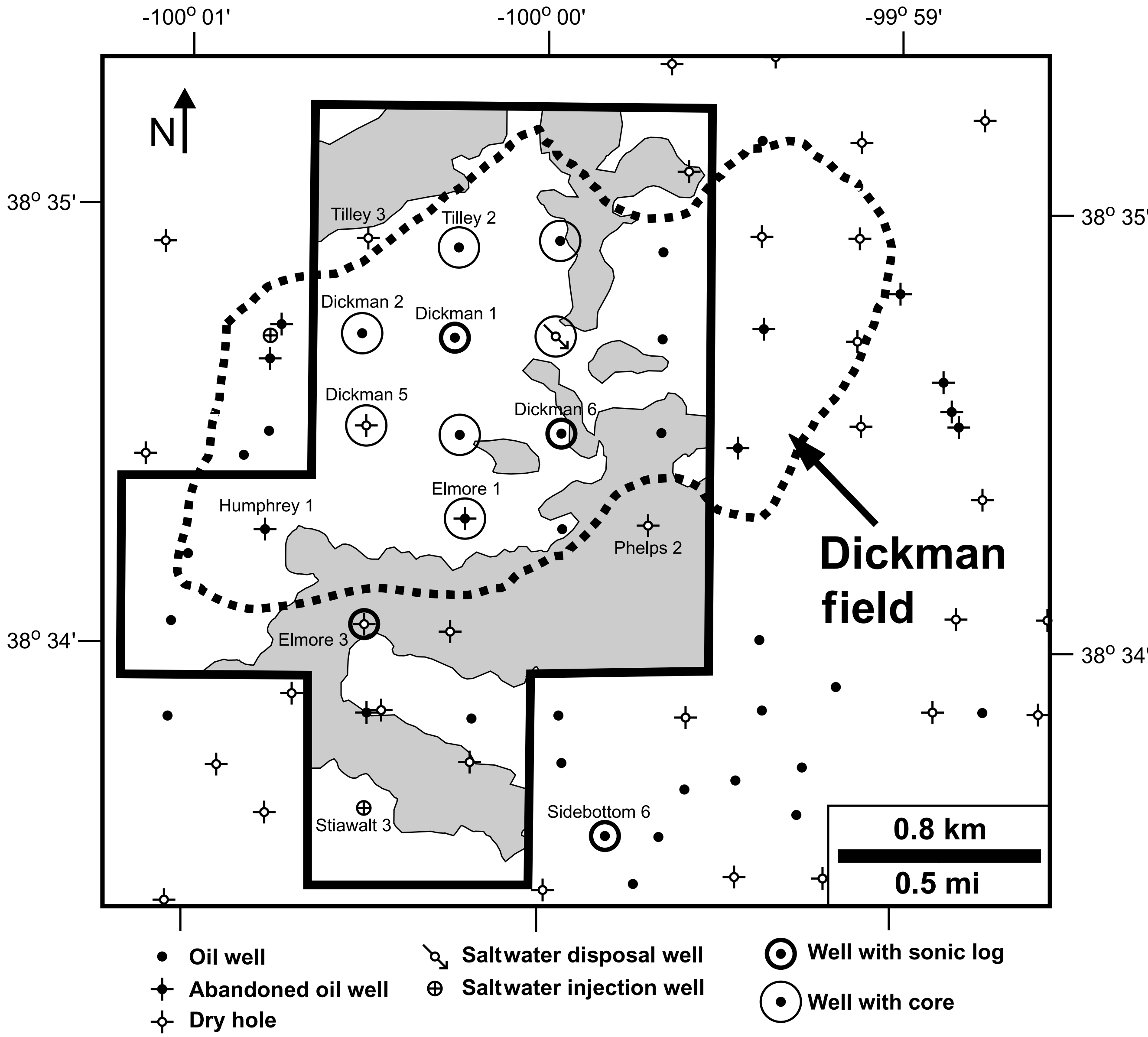

FIGURE 7. Location map of Dickman field (dashed outline) and the Dickman 3-D seismic survey (heavy black outline). The gray shaded overlay indicates areas where the top of the Mississippian, as interpreted from the 3-D seismic volume, is below the oil-water contact.

determined that, although depositional facies and early diagenetic events are the dominant controls on matrix characteristics, reservoir properties have been both enhanced and destroyed by subsequent fracturing and brecciation associated with post-Mississippian karst, burial, and structural events. The depositional, diagenetic, and tectonic history of the Meramecian reservoir in Dickman field is similar to that of the Osagian reservoir in Schaben field, so the same combination of parameters (i.e., original depositional facies plus later fractures) likely controls the reservoir characteristics in Dickman field.

Natural fractures can enhance reservoir permeability, allowing for higher fluid production from the reservoir. However, fractures that have been subsequently filled by a low-permeability material, such as clay, silt, or anhydrite, can serve as barriers to fluid flow, resulting in reservoir compartmentalization.

Carr et al. (2000) interpreted clay- and silt-filled fractures at the top of the Mississippian in a horizontal well from Ness City north field in central Ness County, Kansas (Figure 3), approximately 13 km (8 mi) from the Dickman field study area. In this well, numerous near-vertical clay and silt intervals with apparent widths of up to 5 m (15 ft) occur at intervals of 2–30 m (5–100 ft) along the lateral length of the well. Carr et al. (2000) interpreted these intervals as solution-enhanced fractures

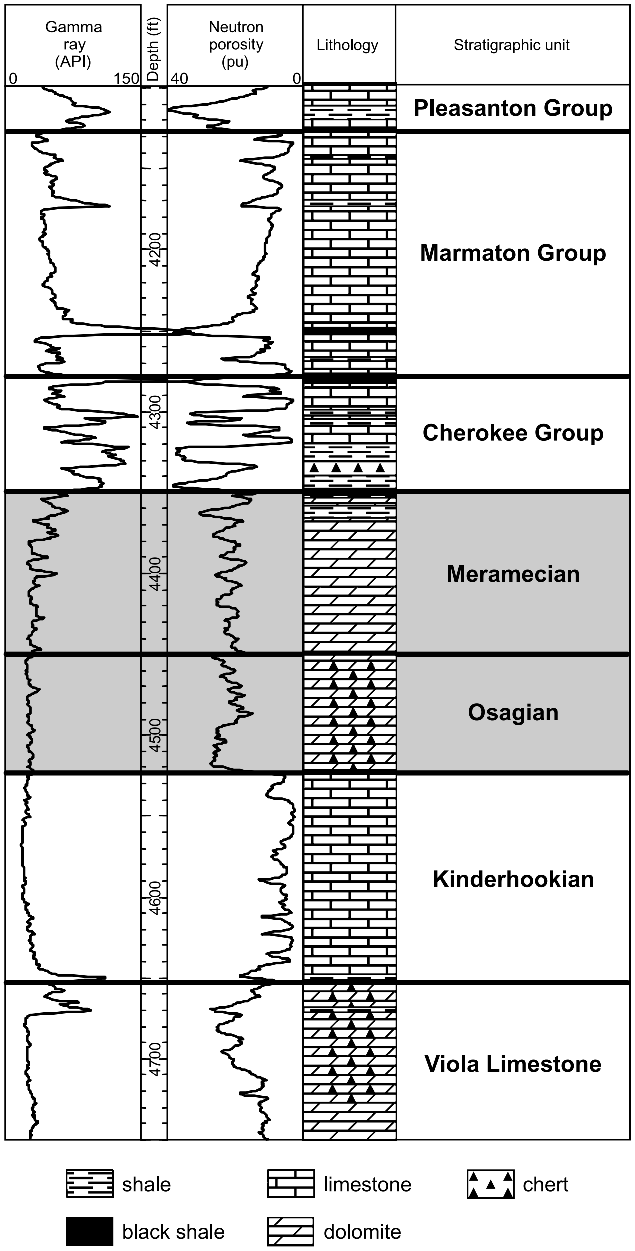

FIGURE 8. Stratigraphic column from the Stiawalt 3 well, just to the south of Dickman field, showing the porous Mississippian dolomite aquifer (gray shading) of the Western Interior Plains aquifer system, which supports the bottom water drive for the Mississippian reservoir in Dickman field.

extending down several meters (tens of feet) or more from the karst surface at the top of the Mississippian that were subsequently filled by transgressive Pennsylvanian clay and silt of the Cherokee Formation. In other Mississippian fields in Kansas, karst-enhanced fractures have been documented to extend several meters below the regional unconformity surface. For example, Ebanks et al. (1977) report shale- and breccia-filled fractures extending 9 m (30 ft) below the pre-Pennsylvanian unconformity surface at Bindley field, 43 km (27 mi) to the south of Dickman field. Therefore, transgression-related fine-grained fill in solution-enlarged fractures can provide a significant barrier to fluid flow in the reservoir, particularly when, as in Dickman field, the entire thickness of the hydrocarbon reservoir extends less than 11 m (35 ft) above the oil-water contact.

METHODOLOGY

Identification of fracture characteristics that affect reservoir performance can be difficult using well data alone. We are unable to define the dimensions and lateral distribution of near-vertical fractures from vertical wells. Even horizontal wells only provide information along a single horizontal path. A 3-D seismic survey is one potential tool for identifying the spatial distribution and trends of major fractures or fissures. We have interpreted key seismic horizons and extracted seismic attributes for a 3-D seismic survey over Dickman field in an attempt to more effectively locate and characterize fractures influencing fluid flow in the Mississippian reservoir.

FIGURE 9. Core scan from 3.7 m (12 ft) below the top of the Mississippian in the Tilley 2 well. The black arrow indicates a small solution-enlarged vertical fracture in the Mississippian dolomite reservoir.

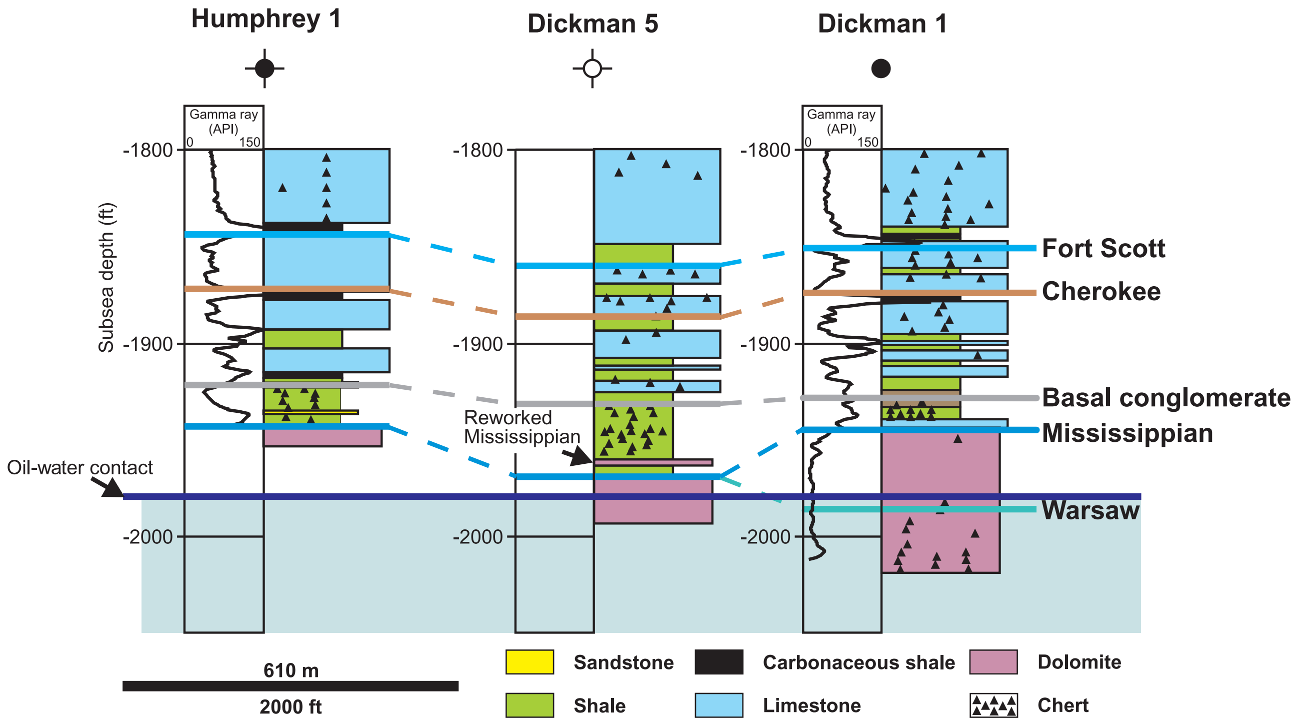

FIGURE 10. Southwest–northeast lithologic cross section through three wells in Dickman field, showing that the top of the Mississippian in the Dickman 5 well is anomalous with respect to surrounding wells.

Conventional Seismic Interpretation

We made detailed structural interpretations within the area of Dickman field using a recently acquired and processed 5 km^2 (2 mi^2) 3-D seismic survey (Figure 7). The seismic data acquisition parameters are shown in Table 1. After stacking onto a natural 33.5- by 25.1-m (110- by 82.5-ft) grid, the data were spatially interpolated in the frequency-x-y (f-x-y) domain to a 25.1- by 25.1-m (82.5- by 82.5-ft) grid, migrated, and spectrally whitened between 20 and 125 Hz.

Three wells within the bounds of the seismic survey and one well 366 m (1200 ft) outside the survey limits included sonic logs, allowing us to construct synthetic seismograms and tie key stratigraphic units to seismic reflections. The synthetic seismograms indicate that the top of the Mississippian roughly corresponds to a seismic peak at the Elmore 3 and Dickman 6 wells, to a position on the flank of the peak at the Dickman 1 well, and near a positive to negative zero crossing below a relatively high amplitude peak at the Sidebottom 6 well (Figure 11). The change in phase along the top of Mississippian reflection appears to be primarily related to variations in the impedance of the overlying Cherokee section. For example, in Sidebottom 6, high-velocity sandstone is present at the base of the Pennsylvanian, and a larger impedance contrast is observed between this sandstone and the overlying shale than between the sandstone and the underlying Mississippian dolomite. This high-velocity sandstone appears to fill a Cherokee valley incised into the Mississippian carbonates (Figure 12A).

The phase change on the top of Mississippian reflection caused by lateral lithology variations makes the Mississippian surface difficult to interpret on the seismic amplitude data. Therefore, we used commercial software to generate a model-based inversion for acoustic impedance, which removed the lateral changes in waveform and tuning. The interface between the lower velocity Pennsylvanian shale, sandstone, or siltstone and the higher velocity Mississippian dolomite appears as an inflection point in acoustic impedance that can be carried across the survey (Figure 13). Nevertheless, it is still difficult to distinguish the high-velocity Pennsylvanian sandstone from the high-velocity Mississippian dolomite.

We combined the top of Mississippian horizon interpreted from the acoustic impedance volume with the

TABLE 1. Seismic acquisition parameters.

Source line orientation	West–east
Source interval	50 m (165 ft)
Source line spacing	268 m (880 ft)
Receiver line orientation	South–north
Receiver interval	67 m (220 ft)
Receiver line spacing	201 m (660 ft)
Sample interval	2.0 ms
Record length	2.0 s

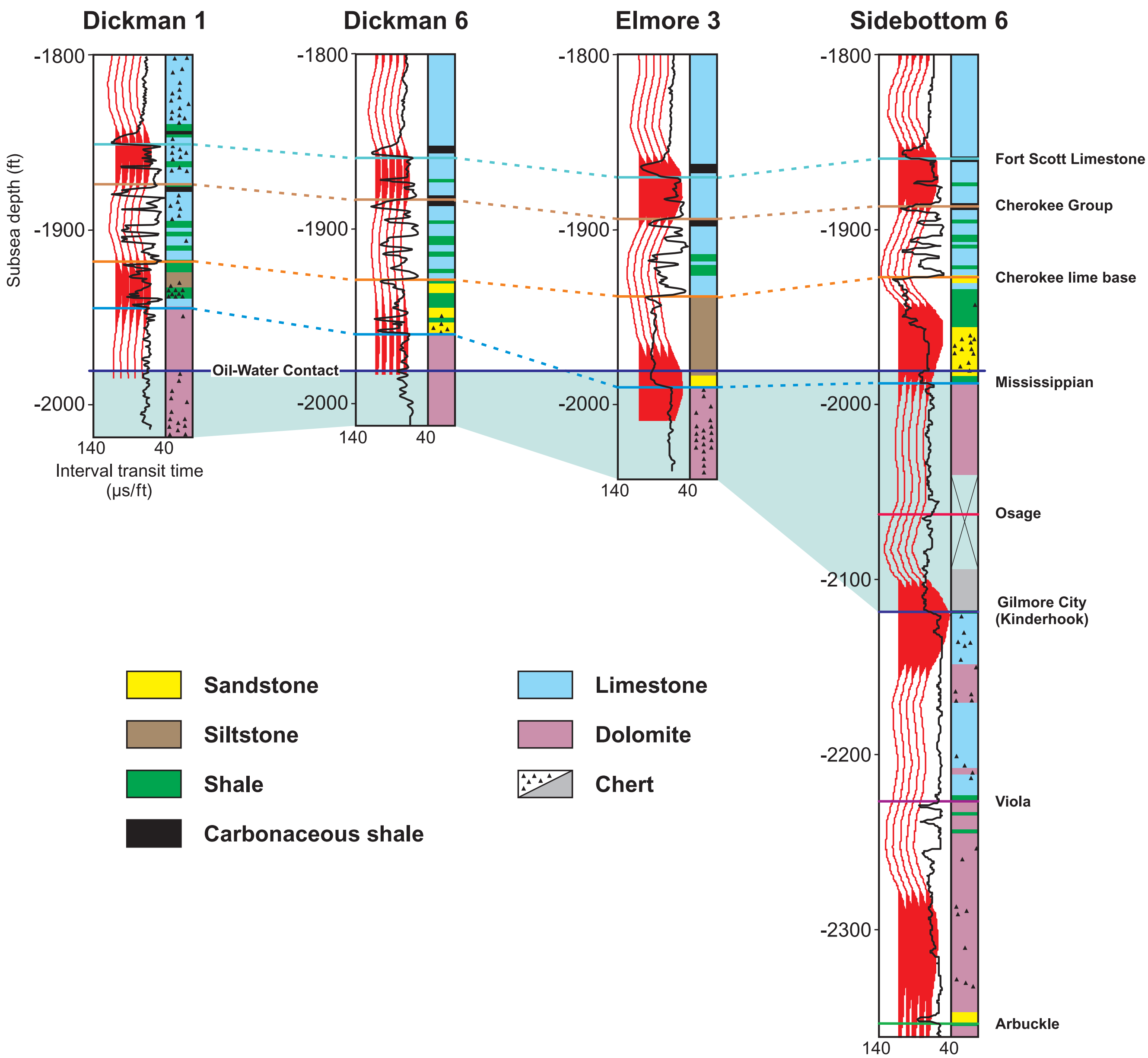

FIGURE 11. Lithologic logs and synthetic seismograms (red) for wells with sonic logs (black) in the Dickman field study area.

well tops to construct a detailed map of the depth to the top of the Mississippian (Figure 12B). This seismic depth map shows topographic detail that is not possible with well data alone (Figure 12A). We used the seismic depth map to refine estimates of the reservoir volume.

The Kinderhookian Gilmore City Limestone that serves as the base of the Mississippian aquifer unit lies approximately 20–30 ms (40–55 m; 130–180 ft) below the reservoir in Dickman field. The Sidebottom 6 synthetic seismogram (Figure 11) shows that the top of the Gilmore City Limestone corresponds to a strong positive seismic reflection, generated from an impedance contrast at the boundary between porous (18% porosity) dolomite above and tight (5% porosity) limestone below. The Gilmore City seismic reflection can be readily interpreted across the entire seismic survey.

The seismic data define the northwestern edge of Dickman field as a down-to-the-north, northeast-trending fault (Figure 13), which corresponds to a lineament on the top of the Mississippian dip map for Ness County (Figure 4A). This northeast-trending lineament and a northwest-trending lineament at the northeastern edge of the seismic survey are the only structural features in Dickman field that are visible on the Ness County Mississippian dip map, which was constructed from well tops. Conventional interpretation of the Dickman 3-D seismic data provides additional structural detail beyond what can be identified using well data alone; however,

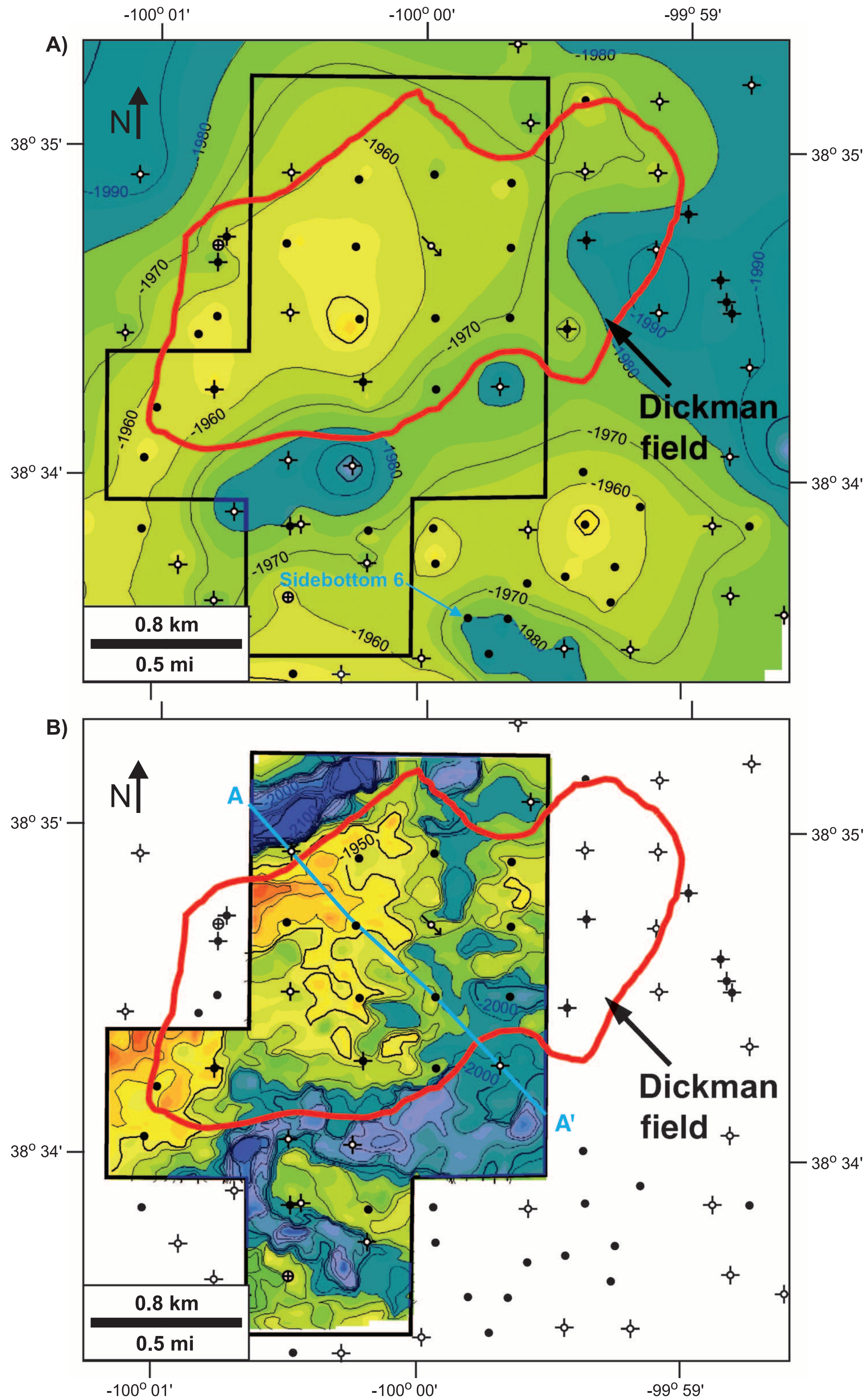

FIGURE 12. Top of Mississippian depth maps from (A) well control only and (B) well control and 3-D seismic survey. Map units are in feet below sea level. The contour interval for both maps is 3 m (10 ft). The blue shading indicates areas where the top of the Mississippian lies beneath the oil-water contact. The location of cross section AA′ in Figure 13 is indicated by the light blue line.

this conventional interpretation is not sufficient for effectively locating fractures that impact fluid flow in the Mississippian reservoir. Advanced seismic attributes such as volumetric curvature provide a method for extracting more information from the seismic data.

Volumetric Curvature and Fracture Identification

Curvature defines how a curve (two dimensions) or a surface (three dimensions) is bent or flexed. The more

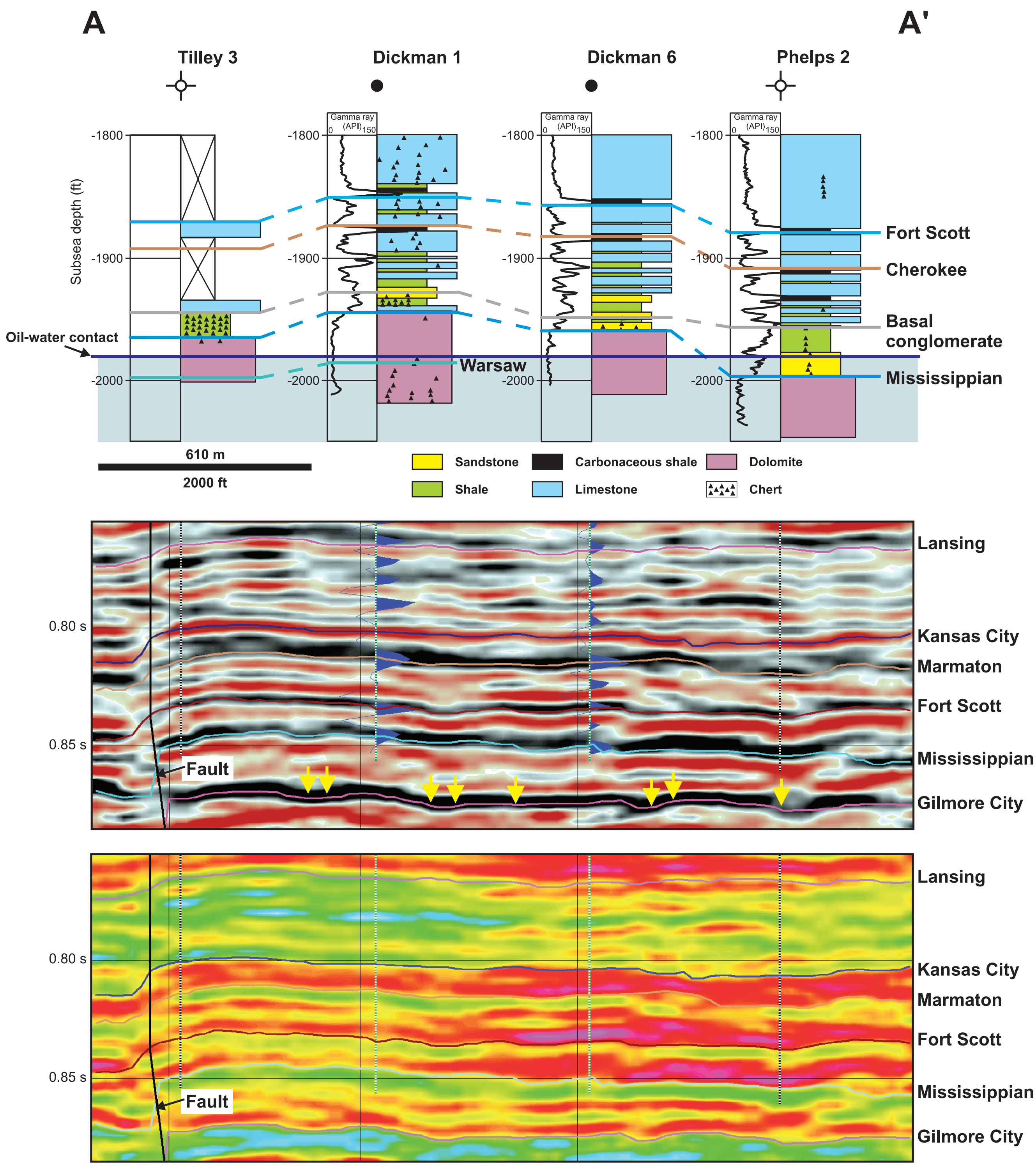

FIGURE 13. Northwest to southeast cross section AA′ across Dickman field, showing (top) lithologic and gamma-ray, (middle) seismic, and (bottom) acoustic impedance data. Key horizons are labeled. Synthetic seismograms calculated from sonic logs in the Dickman 1 and Dickman 6 wells are displayed in blue on the seismic section. Yellow arrows indicate the locations of the lineaments interpreted from the Gilmore City most-negative curvature map in Figure 15. Note that Dickman field is bounded to the northwest by a down-to-the-north fault.

deformed a surface is, the greater its curvature. In two dimensions, positive curvature indicates antiformal, negative curvature synformal, and zero-curvature planar features (Roberts, 2001). In three dimensions, numerous curvature measures can be calculated, depending on the direction of the plane along which curvature is measured. Roberts (2001) showed how these various curvature attributes reveal information about the shape of an interpreted horizon that allows us to map folds, faults, and lineaments contained within the surface.

Most published work of curvature analysis applied to 3-D seismic data has been limited to calculations based on interpreted horizons (e.g., Stewart and Wynn, 2000; Roberts, 2001; Hart et al., 2002; Masaferro et al., 2003; Sigismondi and Soldo, 2003). Modern software implementations of horizon curvature begin by fitting a quadratic surface to a neighborhood of horizon picks. The various curvature measures are computed by taking second derivatives of this quadratic surface. In contrast, volumetric reflector curvature attributes, described by Al-Dossary and Marfurt (2006), are calculated directly from the seismic data volume, with no prior interpretation required. Instead of taking the second derivatives of a picked horizon, Al-Dossary and Marfurt (2006) took first derivatives of volumetric inline and crossline components of reflector dip. Because these dip components are computed from semblance scans within small volumetric (horizontal and vertical) analysis windows (in our case, 9 traces by 20 ms), they are less sensitive to backscattered ground roll and other noise than are interpreter-picked horizons of peaks, troughs, or zero crossings. Al-Dossary and Marfurt (2006) also showed how we can compute volumetric curvature at different wavelengths. Although short-wavelength components of curvature can be computed using as few as 9 traces, long-wavelength components of curvature are computed using 100–200 traces. Such long-wavelength computations enhance subtle, longer wavelength sags and flexures. In addition, using many more traces allows the long-wavelength computations to stack out random errors in the reflector dip estimate. As a result of the above factors, volumetric curvature provides higher quality curvature images than curvature calculated along an interpreted horizon (Figure 14). In addition, volumetric curvature extracted along an interpreted horizon has the benefit of not being as strongly dependent on the quality of the horizon interpretation as curvature that is calculated from the horizon picks.

Volumetric curvature has proven to be useful in improved identification of subtle lineaments that cannot be identified with conventional 3-D seismic attributes, including coherence. This is because fractures or small-offset faults (with vertical offsets less than one-quarter wavelength) will not cause a break in the seismic reflector and, thus, are not detectable by coherence. However, the same fractures and small-offset faults may produce subtle flexures in the seismic reflector that can be detected by volumetric curvature (Figure 14).

Of the numerous volumetric curvatures calculated, the most-positive and most-negative curvatures, which measure the maximum positive (antiformal) and negative (synformal) bending of the surface at a given point, are the most useful for delineating subtle faults, fractures, flexures, and folds (Al-Dossary and Marfurt, 2006; Blumentritt et al., 2006; Sullivan et al., 2006a, b). Solution-enhanced fractures are best imaged using the most-negative curvature volume. The fractures (or, more likely, fracture swarms) appear as lineaments with a high negative curvature value (corresponding to synforms), whereas the surrounding unaltered rocks have a near-zero curvature. One possible explanation is that the fractures are open, locally decreasing the average velocity of the rock and causing a velocity pushdown of the seismic horizon. Similarly, a velocity pushdown could be produced if the fractures are filled with a material such as clay or silt that has a lower velocity than the dolomite host rock. In this case, the softer infill material may also have undergone greater differential compaction than the surrounding rock, warping overlying strata as well as the subject horizon.

We computed a long-wavelength volumetric curvature from the Dickman 3-D seismic volume to illuminate seismic features related to fractures in the Mississippian reservoir. We used a horizontal window of 120 traces (251 × 251 m; 825 × 825 ft) and a vertical window of 20 ms (approximately 40 m [130 ft] at the depth of interest) for our computations. We then extracted maps of most-negative curvature along the top of Mississippian and Gilmore City Limestone seismic horizons. By superimposing these two maps, we are able to recognize the vertical continuity of features through the Mississippian aquifer unit (Figure 15). The two maps are very similar, showing oriented sets of lineaments that appear to persist from the top to the base of the interval. Lineaments with similar orientations are observed in most-negative curvature extractions from horizons above the Mississippian, but the spatial positions and continuity of the lineaments vary, and curvature magnitudes are decreased for shallower horizons.

Topographic irregularities caused by erosion on the top of the Mississippian horizon can modify the shape of the lineaments on the extracted curvature map. Therefore, we traced lineaments on the underlying, smoother, Gilmore City map and analyzed the lineament orientations using rose diagrams (Figure 16).

Figure 16 shows two main orientations, N45°E and N45°W, which are similar to the orientations of lineaments interpreted from the regional dip magnitude map of the top of the Mississippian surface (Figure 4). The orientation is also similar to regional gravity (Figure 5) and magnetic (Figure 6) lineament trends for Ness County, Kansas, both of which indicate basement structural trends.

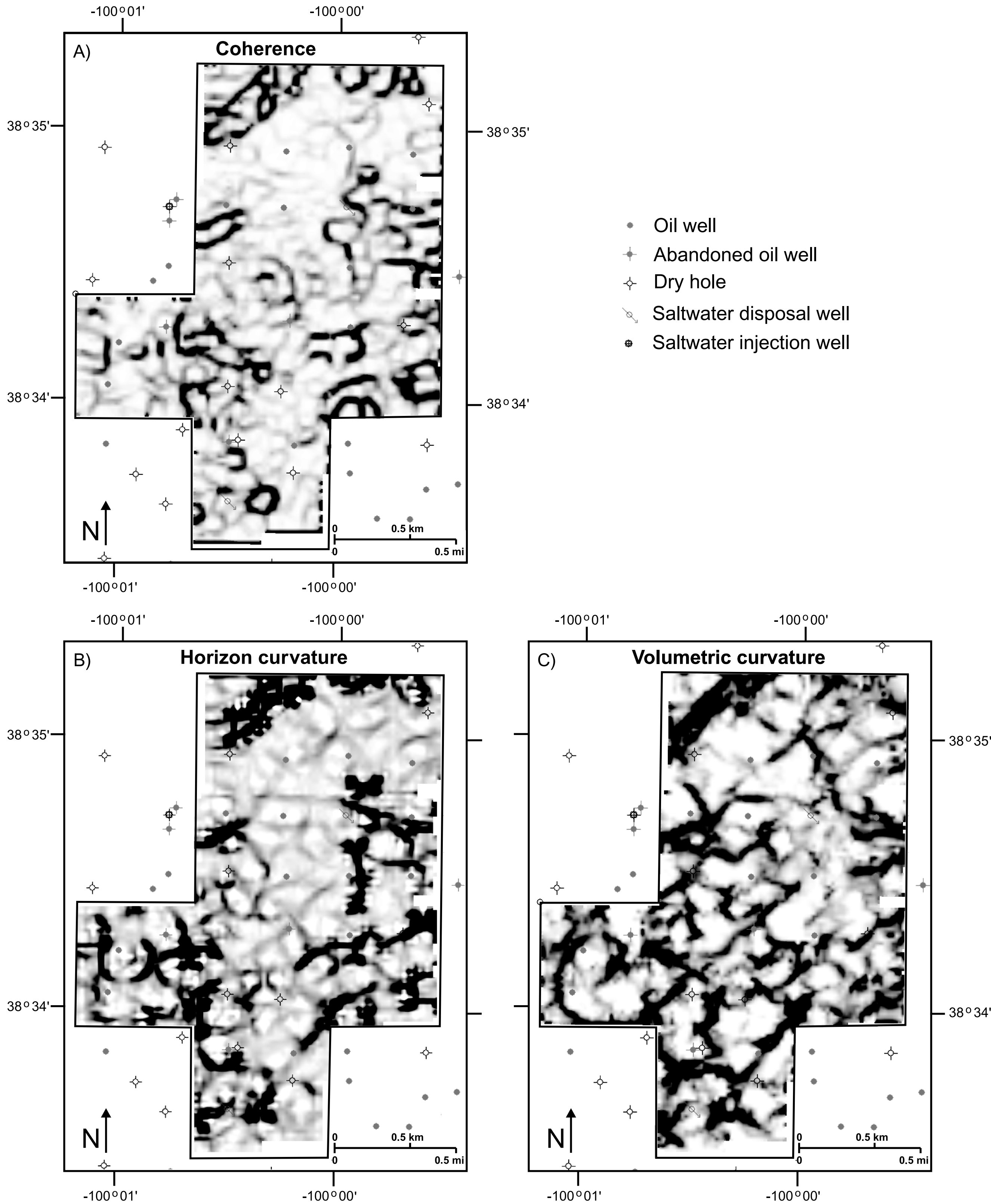

FIGURE 14. Comparison of (A) coherence, (B) most-negative curvature from gridded, interpreted horizon, and (C) extracted volumetric most-negative curvature for the Gilmore City horizon from the Dickman seismic survey. Note that oriented lineaments, which cannot be seen on the coherence map, are visible on the two curvature maps. Also note that the lineaments are better defined on the volumetric curvature map than on the horizon curvature map.

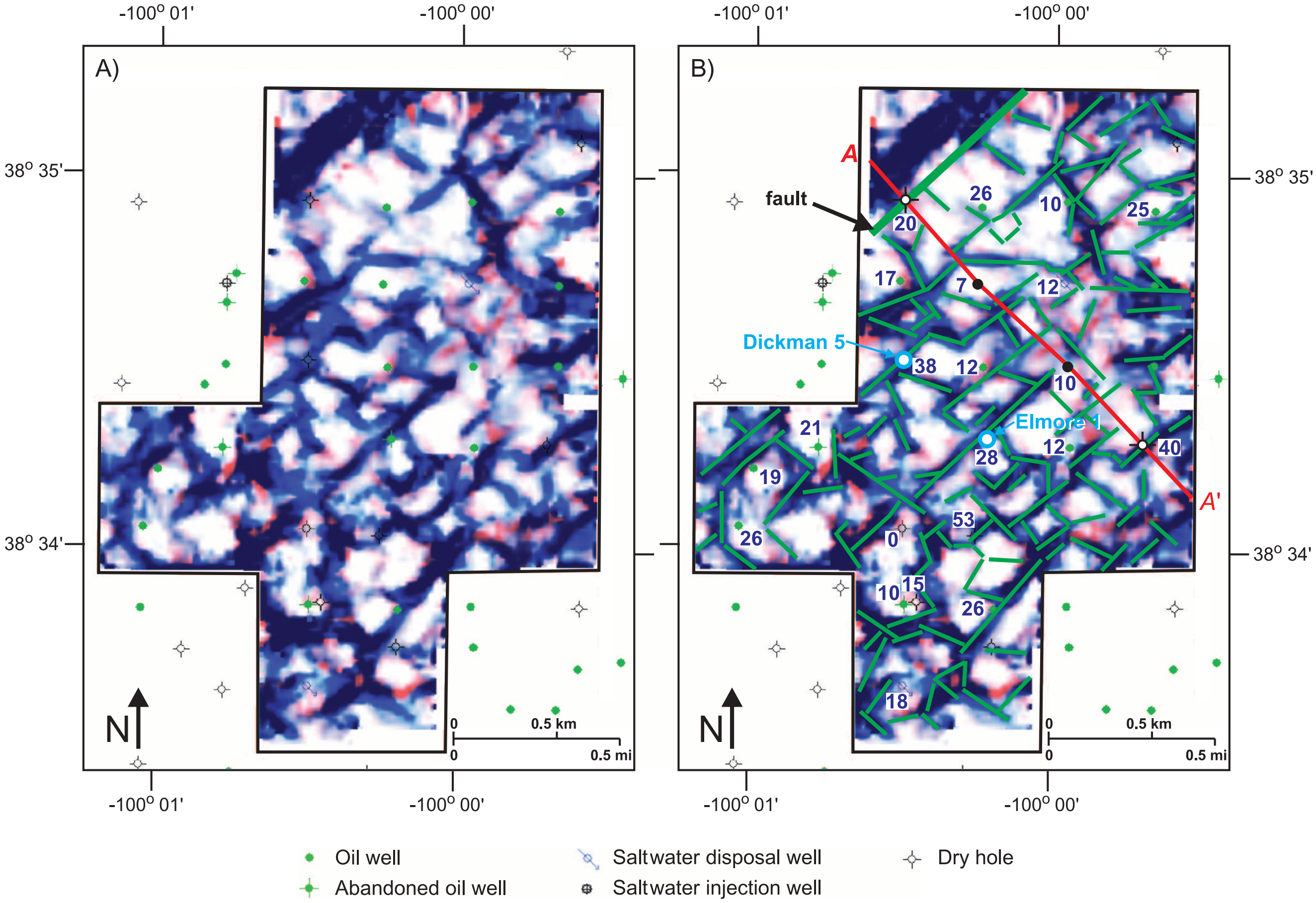

FIGURE 15. Superimposed volumetric most-negative curvature maps extracted at the (red) top of Mississippian and (blue) Gilmore City horizons. Saturated colors indicate the tightest curvature. Purple indicates features that are coincident on the two maps. The uninterpreted composite map is shown in panel A. Lineaments interpreted from the Gilmore City curvature map are superimposed in green on panel B. Dark blue numbers indicate thickness of the karst zone in feet. The location of cross section AA′ in Figure 13 is indicated by the heavy red line.

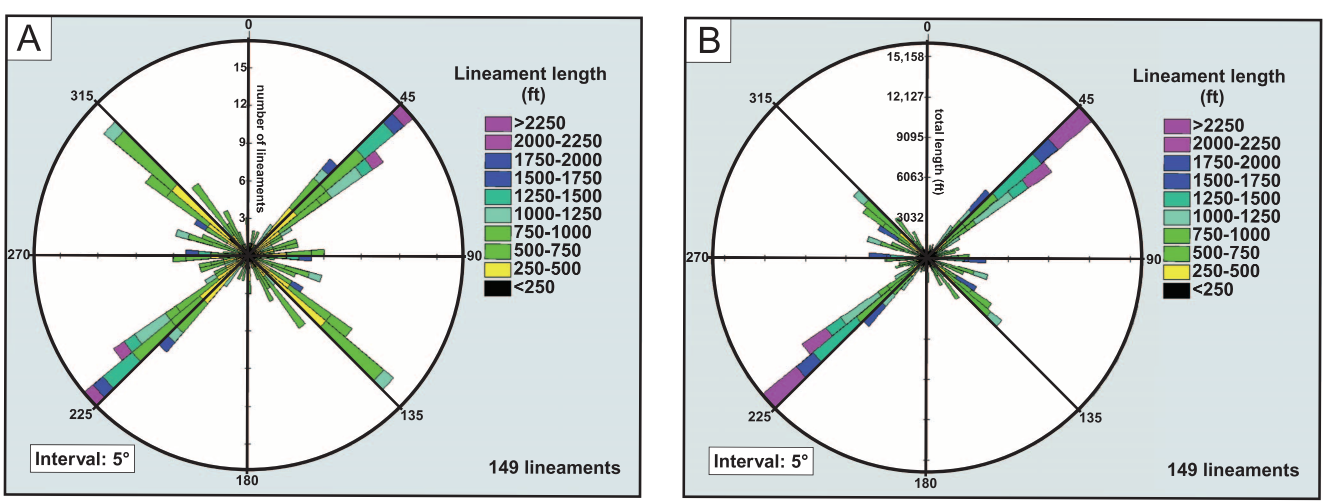

FIGURE 16. (A) Rose diagram showing the number of interpreted lineaments from Figure 15B within a given azimuth sector. Lineament length is indicated by color. (B) Rose diagram showing the sum of lineament lengths from Figure 15B within a given azimuth sector. Lengths of individual lineaments are indicated by color.

We interpret the curvature lineaments as indicators of fracture swarms, potentially solution enhanced, in the Mississippian rocks. The similarity between the orientations of curvature lineaments and basement lineaments suggests that the fracturing of the Mississippian rocks is related to the tectonic reactivation of Precambrian faults, most likely related to north- to northwest-directed compressive stress from the Pennsylvanian Ouachita-Marathon orogeny (Kluth and Coney, 1981; Yarger, 1983; Kluth, 1996).

Although the number of lineaments with northeasterly and northwesterly trends is approximately equal in the Dickman seismic survey, northeast-trending lineaments have greater length and continuity than the northwest-trending lineaments (Figure 16). Also, although lineament spacing for both orientations ranges from 180 to 400 m (600 to 1300 ft), the northeast-trending lineaments are more regularly spaced than the northwest-trending lineaments. The northeast-trending lineaments parallel the fault at the northwest corner of the seismic survey, and the northeast-trending lineaments and the fault are assumed to be genetically related features.

CORRELATION OF CURVATURE TO FLUID FLOW

We correlated our interpreted lineaments to geologic and production data to determine if a relation can be found between the lineaments and fractures that affect fluid flow. Large fractures filled by rock debris and fine-grained sediment can be barriers to fluid flow, whereas open fractures can serve as water conduits from the free-water level below the hydrocarbon reservoir.

We hypothesize that wells penetrating fractures that were solution enhanced by karst and subsequently filled by rock debris will show evidence of a thicker section of weathered Mississippian material at the base of the Pennsylvanian (subsequently referred to as the "karst zone") than the surrounding wells. In this study, we define the karst zone in a well as the interval between the highest occurrence of the basal chert conglomerate in the Pennsylvanian section (chert weathered from the Mississippian) and the top of the unweathered Mississippian, as identified from cuttings and core. In wells where core data are not available, we used the well site geologists' reports to obtain this information.

In general, areas with a thick basal conglomerate are assumed to have been lows in the Pennsylvanian that collected more debris than areas with a thinner or absent basal conglomerate. Variations in the thickness of the basal conglomerate do not appear to have a long-wavelength trend (Figure 15), suggesting that local features, such as solution-enhanced fractures or small sinkholes, are present and have locally influenced the paleotopography.

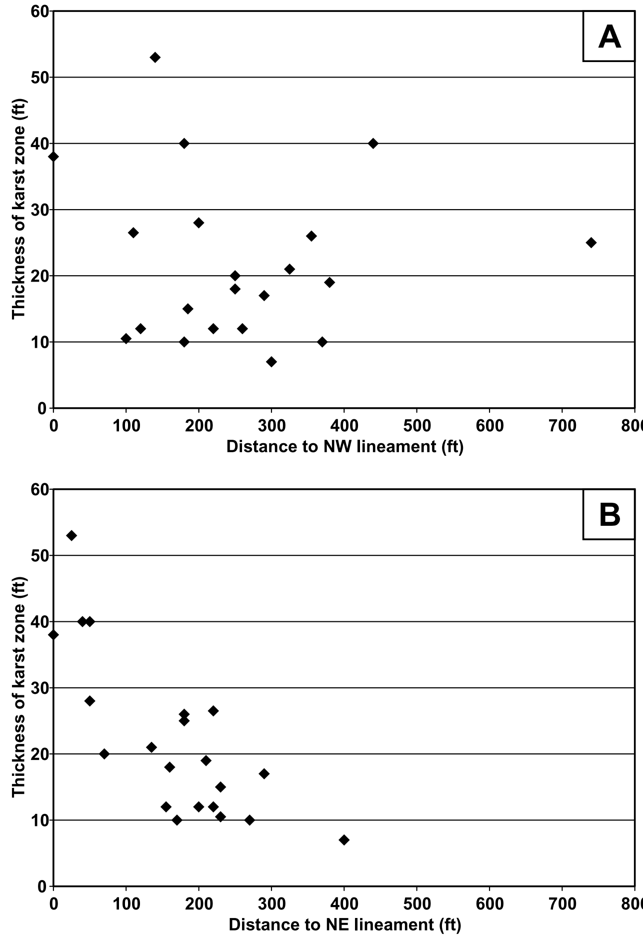

FIGURE 17. Crossplots of the thickness of the karst zone versus distance to (A) northwest-trending and (B) northeast-trending lineaments interpreted from the Gilmore City curvature map. No visual relation between the thickness of the karst zone and the northwest-trending lineaments is seen in panel A. The karst zone thickness increases with proximity to the northeast-trending lineaments in panel B, with the thickest karst zone occurring within 15 m (50 ft) of the northeast-trending lineaments.

To determine whether either of the two dominant lineament trends observed in the volumetric curvature data relate to debris-filled solution-enhanced fractures, we crossplotted the thickness of the karst zone, as defined above, versus the distance to the nearest northeast- and northwest-trending lineaments (Figure 17). Crossplots show that no apparent correlation between the thickness of the karst zone and the northwest-trending lineaments exists (Figure 17A); however, a marked increase in the thickness of the karst zone for wells within 15 m (50 ft) of the northeast-trending lineaments is present (Figure 17B). Correspondingly, two of the three cored wells that we interpreted to be located within large

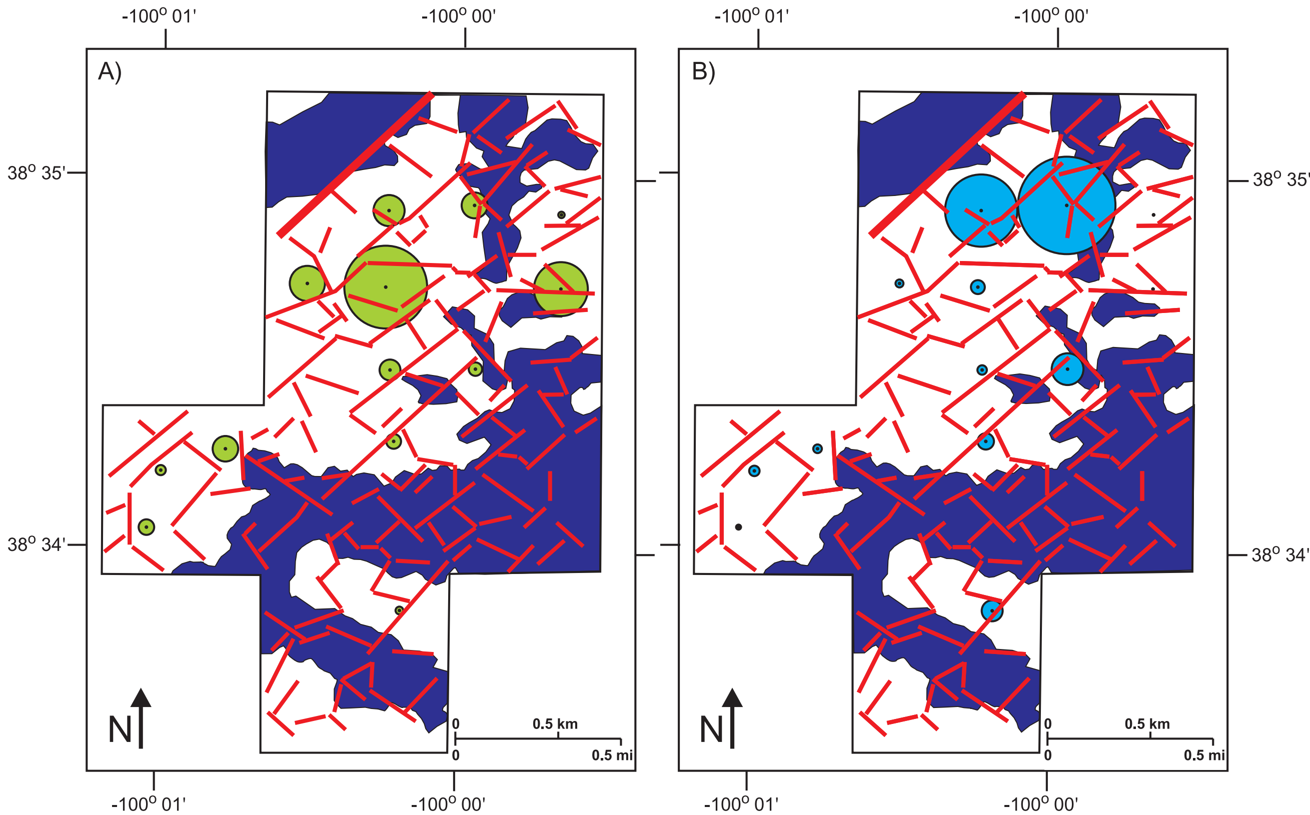

Figure 18. (A) Bubble map showing (green circles) the amount of oil produced during the first 5 yr of production for each well within the Dickman seismic survey. The largest circle corresponds to approximately 117,600 bbl. Interpreted lineaments are shown in red and areas where the top of the Mississippian is below the oil-water contact are shown in dark blue. (B) Bubble map showing (blue circles) the amount of water produced during the first 5 yr of production for each well within the Dickman seismic survey. The largest circle corresponds to approximately 830,500 bbl. Other map elements as in panel A.

(greater than wellbore diameter) debris-filled fractures are situated near northeast-trending curvature lineaments. Dickman 5 sits directly on one of the northeast-trending lineaments and Elmore 1 is located 15 m (50 ft) from another northeast-trending lineament (Figure 15). Of these same three cored wells, only one (Dickman 5, which sits at the intersection between a northwest-trending lineament and a northeast-trending lineament) is located near a northwest-trending lineament.

The correlation between the thickness of the karst zone and distance to the northeast-trending lineaments, supported by evidence from cored wells penetrating debris fill, suggests that northeast-trending lineaments are likely to represent fractures preferentially solution enhanced during karst formation and subsequently filled with clay, silt, and other debris. Because some of the northeast-trending lineaments have interpreted lengths in excess of 0.8 km (0.5 mi), they may provide significant barriers to fluid flow in the northwest–southeast direction.

The correlation between the interpreted lineaments and fluid flow was investigated directly by examining the spatial variability of fluid production from the wells in Dickman field in relation to lineament proximity. Bubble maps of oil production and water production (Figure 18) show no obvious spatial relation for wells with high oil or water production as compared to wells with low oil or water production. To evaluate whether a link between oil production and lineament orientation exists, oil production was crossplotted against the distance to the nearest northeast- and northwest-trending lineaments (Figure 19). The crossplots indicate that no identifiable relation exists between oil production and the northwest-trending lineaments (Figure 19A), but an overall increase in oil production is present with increasing distance from the northeast-trending lineaments (Figure 19B). This suggests that oil production is inhibited in proximity to the northeast-trending lineaments, where there may be a higher concentration of low-permeability debris-filled fractures.

The bottom of the interval open for production in the Dickman field wells ranges from 1 to 7 m (3 to 24 ft) above the oil-water contact. Capillary pressure analysis of samples from the Tilley 2 core indicates that, for the reservoir in Dickman field, the hydrocarbon column is

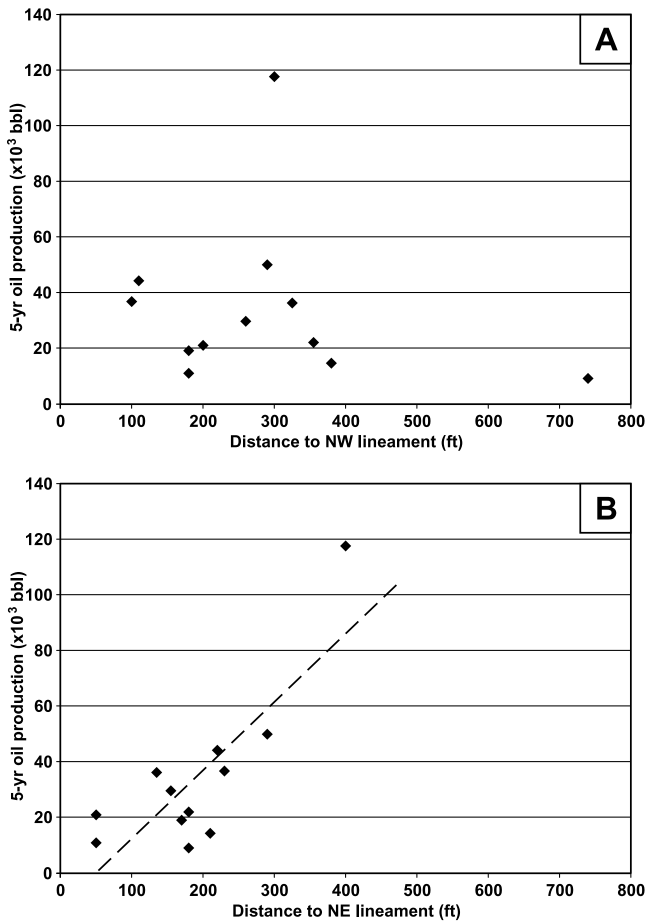

FIGURE 19. Crossplots of 5-yr oil production versus distance to (A) northwest-trending and (B) northeast-trending lineaments interpreted from the Gilmore City curvature map. No identifiable relation between oil production and the northwest-trending lineaments is seen in panel A. Oil production increases with distance from the northeast-trending lineaments in panel B. The dashed line shows a linear least squares fit to the data.

within the capillary transition zone, even for the highest part of the field at 11 m (35 ft) above the oil-water contact (Alan Byrnes, 2006, personal communication). Although height above the oil-water contact and porosity and permeability appear to be contributing factors in the amount of water produced from these wells, several wells have higher water production than can be explained by matrix porosity and permeability alone, without invoking another mechanism for fluid flow.

Water production from Dickman field wells may be related to open fractures that extend into the underlying Mississippian aquifer. To evaluate whether open fractures are preferentially linked to lineament orientation, we crossplotted water production against the distance to the nearest northeast- and northwest-trending lineaments (Figure 20). The crossplots show no visible correlation between water production and the northeast-trending lineaments (Figure 20B); however, increased water production with closer proximity to the northwest-trending lineaments is observed (Figure 20A). A power, law function provides a good fit to this relation. These results suggest that the northwest-trending lineaments represent currently open fractures, which serve as conduits to the aquifer.

DISCUSSION

In Dickman field, 3-D seismic volumetric curvature attributes reveal two lineament directions, northeast and northwest, reflecting regional structural trends. The northeast-trending lineaments, which we interpret as sets of solution-enhanced fractures filled with debris and

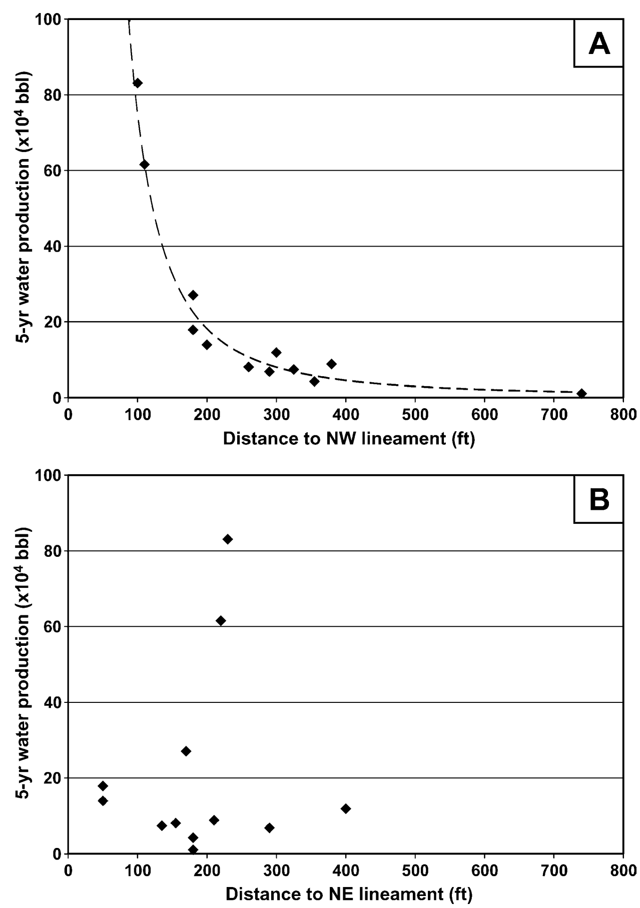

FIGURE 20. Crossplots of 5-yr water production versus distance to (A) northwest-trending and (B) northeast-trending lineaments interpreted from the Gilmore City curvature map. Water production decreases with distance from the northwest-trending lineaments in panel A. The dashed line shows a power-law fit to the data. No identifiable relation between oil production and the northeast-trending lineaments is seen in panel B.

low-permeability clay and silt, appear to be barriers to fluid flow, whereas the northwest-trending lineaments appear to represent open fractures, serving as conduits into the underlying aquifer.

The relative age of the two lineament directions is unknown, and whether the lineaments were formed at the same time or in a succession of events is unclear. The fault on the northwest side of the field apparently had motion throughout the Paleozoic, with early motion interpreted as down to the south, followed by a later (post-Mississippian) reversal of motion (Watney et al., 2008). This indicates that northeast-trending features related to the fault were most likely formed coincident with deposition of the Mississippian and may be related to the reactivation of even older features.

Ancestral Rocky Mountain tectonism, which began during the late Mississippian and extended into the Early Permian, produced many large uplifts, including the Central Kansas uplift and the Nemaha Ridge (Goebel, 1966; Kluth, 1996). The Ancestral Rocky Mountain tectonism is linked to the Ouachita-Marathon orogeny, produced by the collision of North America and South America-Africa (Kluth and Coney, 1981). Yarger (1983) noted that Precambrian faults associated with the north-northeast-trending central North American rift system were likely reactivated during Mississippian deformation.

Folding parallel to northeast-trending faults, resulting from north- to northwest-directed compression during the early Pennsylvanian, may have opened preexisting northeast-trending fractures in the Mississippian rocks, allowing fluid flow and solution enhancement of these fractures. The solution-enhanced fractures were subsequently filled by debris and middle Pennsylvanian transgression-related fine-grained sediments of the Cherokee Group.

Because the fractures associated with the northwest-trending lineaments do not appear to have been filled with Pennsylvanian clay and silt, these fractures must either be younger than the middle Pennsylvanian or older fractures that were closed during the early to middle Pennsylvanian. Gerhard (2004) proposed that northwest-trending faults associated with the Nemaha Ridge and extending to the Central Kansas uplift represent the pre-Phanerozoic wrench fracturing of the Kansas crust, indicating that the northwest-trending lineaments may indeed be Precambrian features. The most-negative curvature map of the Gilmore City Limestone shows several northwest-trending lineaments that truncate at, and appear to be offset along, northeast-trending lineaments, suggesting that the northwest-trending lineaments predate the northeast-trending lineaments. The correlation between northwest-trending lineaments and current water production suggests that northwest-trending fractures are open at present. This implies that the present-day maximum horizontal compressive stress in the area is at a low angle to these lineaments. However, Laubach et al. (2004) indicated that the direction of present-day maximum horizontal compressive stress does not necessarily coincide with the direction of open natural fractures in the subsurface; instead, chemical alteration and cementation patterns may provide more control on which fractures are open to fluid flow.

CONCLUSIONS

The widespread Western Interior Plains aquifer system provides significant potential for sequestration of CO_2 in a deep saline formation. This aquifer system also exhibits subtle karst-related features, including debris- and clay-filled solution-enhanced fractures, which could impact compartmentalization and transport of stored CO_2.

Volumetric curvature computed from 3-D seismic volumes provides excellent images of linear synformal features that appear to represent fractures or fracture swarms. In particular, long-wavelength volumetric curvature highlights subtle fracture-related lineaments that cannot be identified by other methods. The integration of curvature and well information provides an insight into the nature of the fractures (fluid conduits versus fluid barriers).

We have developed what we feel to be a novel work flow in correlating seismically imaged fractures to fluid production. Multivariate statistics, geostatistical analyses, and neural networks are routinely used to predict reservoir properties, such as porosity thickness, by relating log- or core-based measurements to seismic attribute values at well locations. These workflows are not readily generalized to predict open and sealed fractures from volumetric curvature because the curvature magnitude at the well location does not necessarily correlate with the presence or absence of fractures in the well and provides no information on the nature of these fractures. We find that the proximity of the well to a curvature lineament is a better indicator of the presence or absence of fractures, and that the nature of the fractures appears to vary azimuthally, most likely caused by the impacts of paleostress and diagenesis, coupled with present-day stress directions. Our interpretation work flow consists of first extracting the volumetric curvature along a horizon of interest. We interpret curvature lineaments on this map and then subdivide the interpreted lineaments into azimuthally limited sets. For each azimuthally limited lineament set, we measure the distances between the wells and the nearest lineaments and correlate these distances with fluid production. Comparing results from the different azimuths allows us to better understand if preferential orientations of open and sealed fractures exist.

We find that 3-D seismic volumetric curvature provides a potentially powerful tool for more effectively locating and characterizing fractures influencing fluid retention and flow in depleted oil and gas reservoirs and aquifers. Advanced seismic attributes, such as volumetric curvature, that can improve the imaging of fractures within and above the reservoirs and aquifers are invaluable for the selection and characterization of geological CO_2 sequestration sites. Attribute-based fracture imaging can be used to evaluate seal integrity, to maximize injection and storage of sequestered CO_2, and to minimize early breakthrough between wells where CO_2 is being used for enhanced oil recovery.

ACKNOWLEDGMENTS

The authors would like to thank the Grand Mesa Operating Company for providing seismic and well data and Seismic Micro-Technology, Inc., Hampson-Russell Limited Partnership, and IHS Corporation for access to software. Rose diagrams were constructed with GEOrient software, courtesy of R. J. Holcombe, Holcombe Coughlin & Associates Australia (http://www.holcombe.net.au/software/). This work was conducted while the authors were with the Kansas Geological Survey, University of Kansas (Nissen and Carr), and the Allied Geophysical Laboratories, University of Houston (Marfurt and Sullivan). The support of these institutions is gratefully acknowledged. Funding for this work was provided by the U.S. Department of Energy under contracts DE-FG26-03NT15438, DE-FC26-04NT15504, and DE-FG26-06NT42734.

REFERENCES CITED

Al-Dossary, S., and K. J. Marfurt, 2006, 3-D volumetric multispectral estimates of reflector curvature and rotation: Geophysics, v. 71, p. P41–P51.

Bhattacharya, S., M. K. Dubois, A. P. Byrnes, S. E. Nissen, T. R. Carr, E. K. Franseen, M. Shreve, S. Anderson, P. M. Gerlach, and B. Knoll, 2005, Field demonstration of horizontal infill drilling using cost-effective integrated reservoir modeling—Mississippian carbonates, central Kansas: Kansas Geological Survey, Open-File Report 2005-28: http://www.kgs.ku.edu/PRS/publication/2005/OFR04_28/ (accessed July 16, 2007).

Blumentritt, C. H., K. J. Marfurt, and E. C. Sullivan, 2006, Volume based curvature computations illuminate fracture orientations—Early to mid Paleozoic, Central Basin platform, west Texas: Geophysics, v. 71, p. B159–B166.

Cansler, J. R., 2000, Paleogeomorphology of the sub-Pennsylvanian unconformity on the Arbuckle Group (Cambrian–Lower Ordovician): Master's thesis, University of Kansas, Lawrence, 123 p. (available as Kansas Geological Survey, Open-File Report 2000-82).

Carr, T. R., 1994, Kansas oil and gas production trends: Kansas Geological Survey, Open-File Report 94-11, 9 p.

Carr, T. R., S. Bhattacharya, and R. Pancake, 2000, Horizontal drilling in Kansas: A case history: http://www.kgs.ku.edu/Workshops/Horz2000/R640/ (accessed July 16, 2007).

Ebanks, W. J., R. M. Euwer, and D. E. Nodine-Zeller, 1977, Mississippian combination trap, Bindley field, Hodgeman County, Kansas: AAPG Bulletin, v. 61, p. 309–330.

Franseen, E. K., T. R. Carr, W. J. Guy, and S. D. Beaty, 1998, Significance of depositional and early diagenetic controls on architecture of a karstic-overprinted Mississippian (Osagian) reservoir, Schaben field, Ness County, Kansas (abs.): AAPG Annual Meeting Expanded Abstracts, 6 p., CD-ROM.

Friedmann, S. J., and V. W. Stamp, 2006, Teapot Dome: Characterization of a CO_2-enhanced oil recovery and storage site in eastern Wyoming: Environmental Geosciences, v. 13, p. 181–199.

Gerhard, L. C., 2004, A new look at an old petroleum province: Kansas Geological Survey, Current Research in Earth Sciences, Bulletin 250, pt. 1, 27 p.: http://www.kgs.ku.edu/Current/2004/Gerhard/index.html (accessed July 16, 2007).

Goebel, E. D., 1966, Stratigraphy of Mississippian rocks in western Kansas: Ph.D. dissertation, University of Kansas, Lawrence, 380 p.

Hart, B. S., R. A. Pearson, and G. C. Rawling, 2002, 3-D seismic horizon-based approaches to fracture-swarm sweet spot definition in tight-gas reservoirs: The Leading Edge, v. 21, p. 28–35.

Holtz, M. H., P. K. Nance, and R. J. Finley, 1999, Reduction of greenhouse gas emissions through underground CO_2 sequestration in Texas oil and gas reservoirs: University of Texas at Austin, Bureau of Economic Geology, Final Report, prepared for EPRI through the U.S. Department of Energy, under contract no. WO4603-04: http://www.beg.utexas.edu/environqlty/abndnhydrores/co2text.pdf (accessed August 19, 2007).

Jorgensen, D. G., 1989, Paleohydrology of the central United States: U.S. Geological Survey Bulletin 1989-D, 32 p.

Jorgensen, D. G., J. O. Helgesen, and J. L. Imes, 1993, Regional aquifers in Kansas, Nebraska, and parts of Arkansas, Colorado, Missouri, New Mexico, Oklahoma, South Dakota, Texas, and Wyoming—Geohydrologic framework: U.S. Geological Survey Professional Paper 1414-B, 72 p.

Jorgensen, D. G., J. O. Helgesen, D. C. Signor, R. B. Leonard, J. L. Imes, and S. C. Christenson, 1996, Analysis of regional aquifers in the central Midwest of the United States in Kansas, Nebraska, and parts of Arkansas, Colorado, Missouri, New Mexico, Oklahoma, South Dakota, Texas, and Wyoming—Summary: U.S. Geological Survey Professional Paper 1414-A, 67 p.

Kansas Geological Survey, 2008, Wells with tops available online: http://www.kgs.ku.edu/Magellan/Tops (accessed November 16, 2008).

Kluth, C. F., 1996, Plate tectonics of the Ancestral Rocky Mountains, *in* J. A. Peterson, ed., Paleotectonics and sedimentation in the Rocky Mountain region, United States: AAPG Memoir 41, p. 353–369.

Kluth, C. F., and P. J. Coney, 1981, Plate tectonics of the Ancestral Rocky Mountains: Geology, v. 9, p. 10–15.

Kruger, J. M., 1997, On-line gravity and magnetic maps of Kansas: Kansas Geological Survey Open-File Reports 96-51 and 97-72: http://www.kgs.ku.edu/PRS/PotenFld/potential.html (accessed July 16, 2007).

Lam, C.-K., and H. L. Yarger, 1989, State gravity map of Kansas, *in* D. W. Steeples, ed., Geophysics in Kansas: Kansas Geological Survey, Bulletin 226, p. 185–196.

Laubach, S. E., J. E. Olson, and J. F. W. Gale, 2004, Are open fractures necessarily aligned with maximum horizontal stress?: Earth & Planetary Science Letters, v. 222, p. 191–195.

Loucks, R. G., P. K. Mescher, and G. A. McMechan, 2004, Three-dimensional architecture of a coalesced, collapsed-paleocave system in the Lower Ordovician Ellenburger Group, central Texas: AAPG Bulletin, v. 88, p. 545–564.

Masaferro, J. L., M. Bulnes, J. Poblet, and N. Casson, 2003, Kinematic evolution and fracture prediction of the Valle Morado structure inferred from 3-D seismic data, Salta province, northwest Argentina: AAPG Bulletin, v. 87, p. 1083–1104.

Merriam, D. F., 1963, The geologic history of Kansas: Kansas Geological Survey, Bulletin 162, 317 p.

Montgomery, S. L., E. K. Franseen, S. Bhattacharya, P. Gerlach, A. Byrnes, W. Guy, and T. R. Carr, 2000, Schaben field, Kansas: Improving performance in a Mississippian shallow-shelf carbonate: AAPG Bulletin, v. 84, p. 1069–1086.

Nodine-Zeller, D. E., 1981, Karst-derived early Pennsylvanian conglomerate in Ness County, Kansas: Kansas Geological Survey, Bulletin 222, 30 p.

Roberts, A., 2001, Curvature attributes and application to 3-D interpreted horizons: First Break, v. 19, p. 85–99.

Sigismondi, M. E., and J. C. Soldo, 2003, Curvature attributes and seismic interpretation: Case studies from Argentina basins: The Leading Edge, v. 22, p. 1122–1126.

Stewart, S. A., and T. J. Wynn, 2000, Mapping spatial variation in rock properties in relationship to scale-dependent structure using spectral curvature: Geology, v. 28, p. 691–694.

Sullivan, E. C., K. J. Marfurt, A. Lacazette, and M. Ammerman, 2006a, Application of new seismic attributes to collapse chimneys in the Fort Worth Basin: Geophysics, v. 71, p. B111–B119.

Sullivan, E. C., S. Nissen, and K. J. Marfurt, 2006b, Application of volumetric 3-D seismic attributes to reservoir characterization of karst-modified reservoirs, *in* R. M. Slatt, N. C. Rosen, M. Bowman, J. Castagna, T. Good, R. Loucks, R. Latimer, M. Scheihing, and R. Smith, eds., Reservoir characterization: Integrating technology and business practices: 26th Annual Gulf Coast Section SEPM Foundation Bob F. Perkins Research Conference Proceedings, p. 409–428.

U.S. Department of Energy, 2007, Carbon sequestration technology roadmap and program plan 2007: http://www.netl.doe.gov/publications/carbon_seq/project%20portfolio/2007/2007Roadmap.pdf (accessed August 19, 2007).

Watney, W. L., E. K. Franseen, A. P. Byrnes, and S. E. Nissen, 2008, Evaluating structural controls on the formation and properties of Carboniferous carbonate reservoirs in the northern Midcontinent, U.S.A., *in* J. Lukasik and T. Simo, eds., Controls on carbonate platform and reef development: SEPM Special Publication 89, p. 125–145.

White, D. J., G. Burrowes, T. Davis, Z. Hajnal, K. Hirsche, I. Hutcheon, E. Majer, B. Rostron, and S. Whittaker, 2004, Greenhouse gas sequestration in abandoned oil reservoirs: The International Energy Agency Weyburn pilot project: GSA Today, v. 14, no. 7, p. 4–10.

Yarger, H. L., 1983, Regional interpretation of Kansas aeromagnetic data: Kansas Geological Survey, Geophysics Series 1, 35 p.